



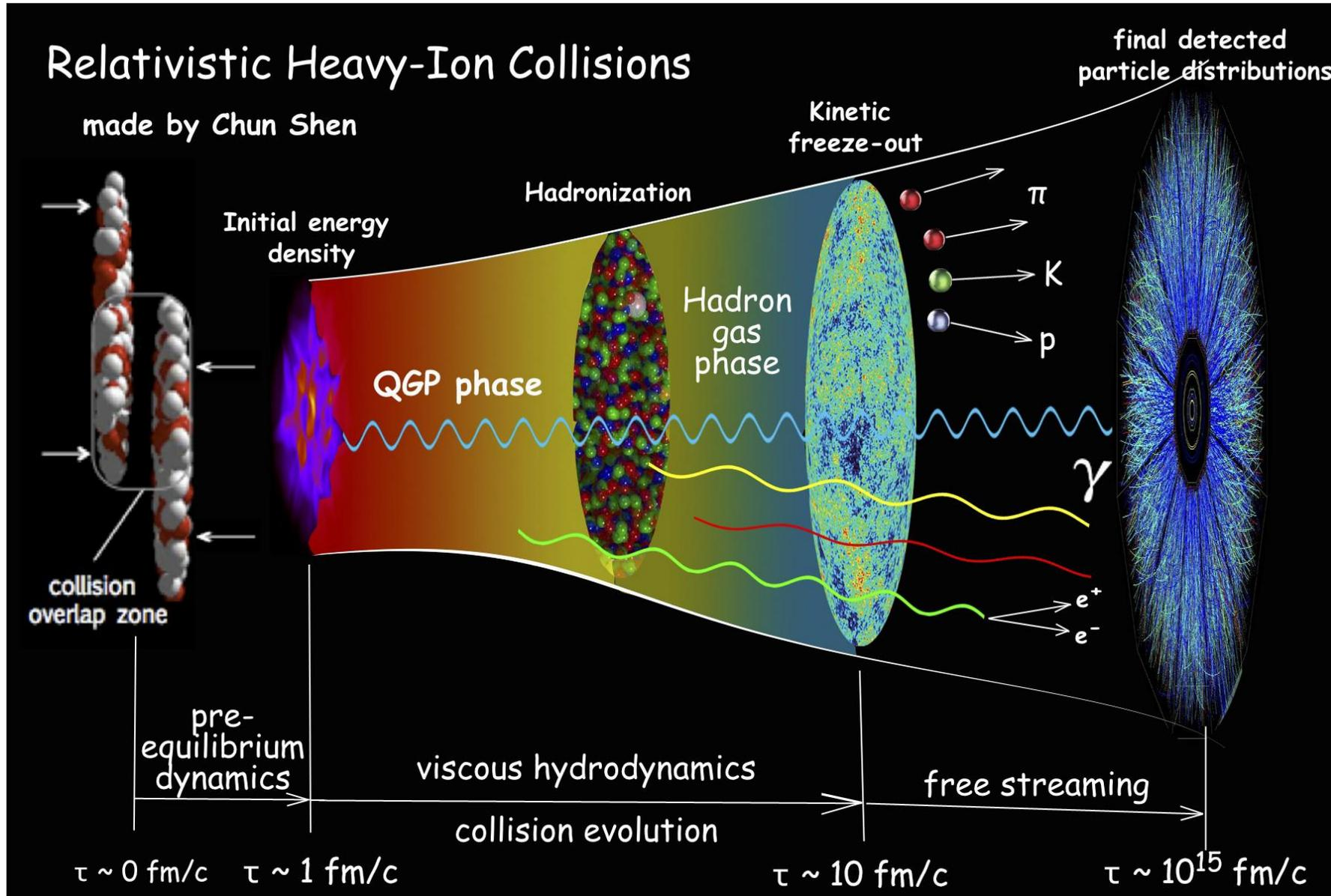
北京大学
PEKING UNIVERSITY

Collectivity & QGP signals in Large and Small systems

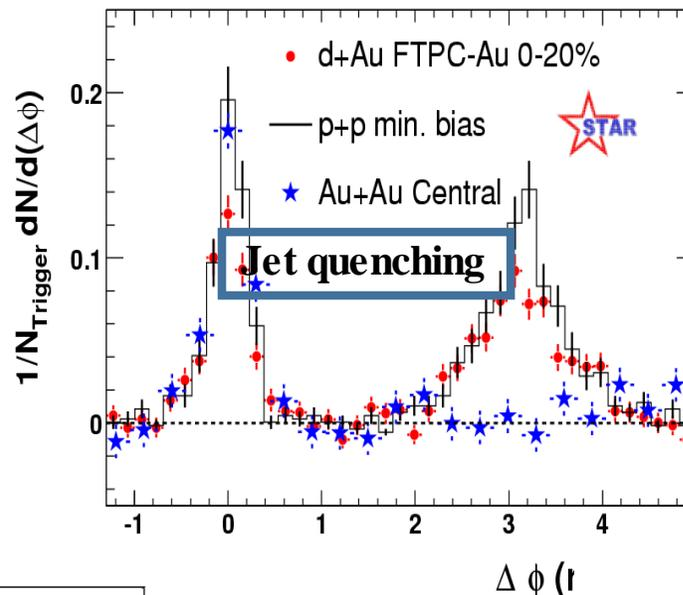
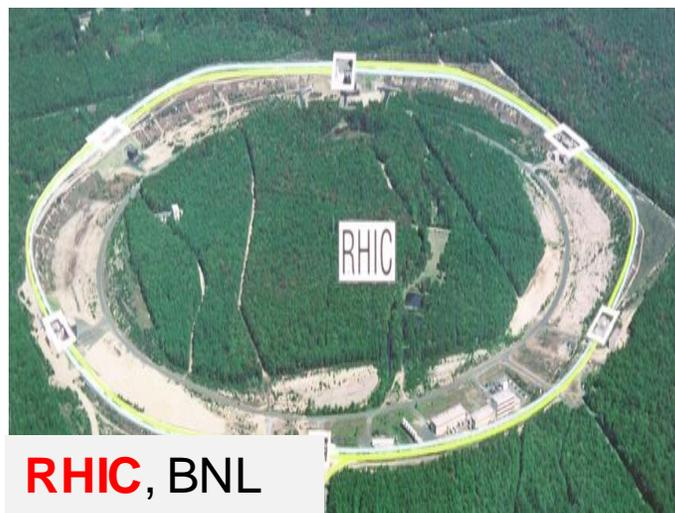
Wenbin Zhao
Peking University

at HENPIC online seminar
June 4, 2020

Illustration of heavy-ion collisions

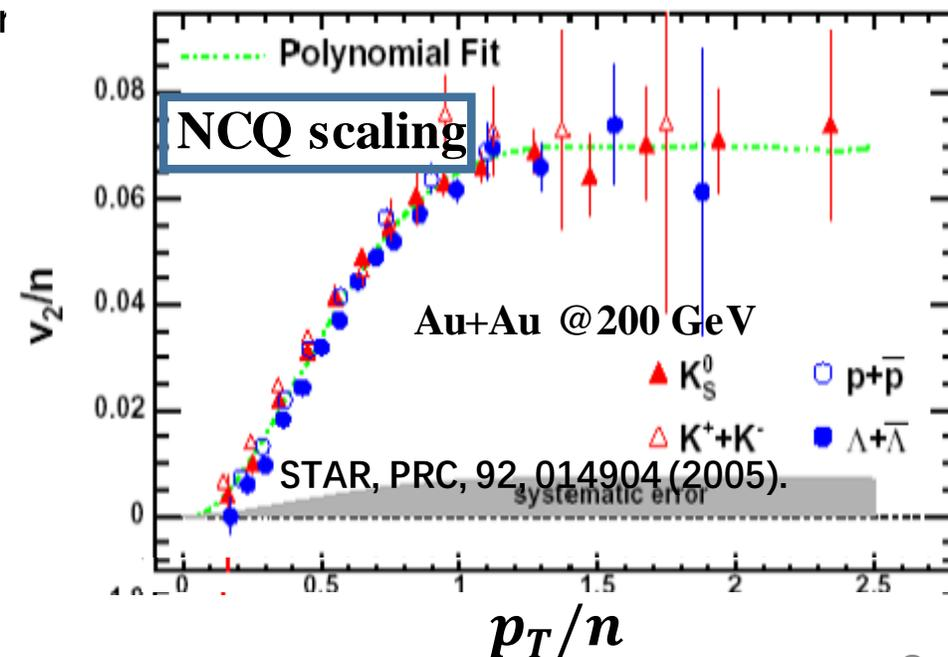
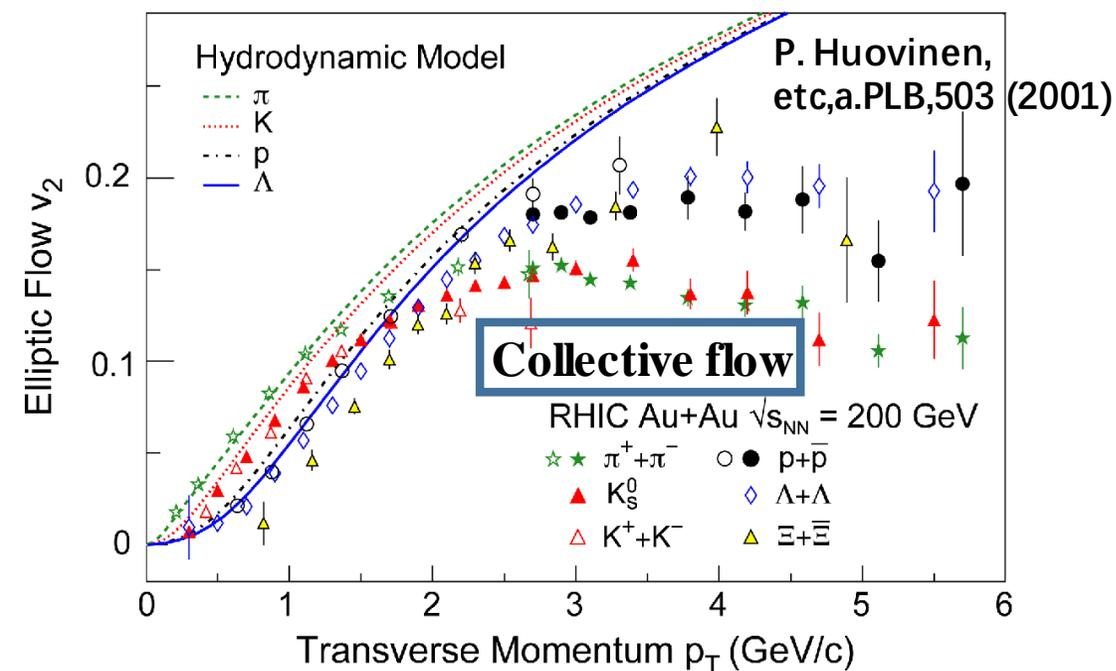


QGP signatures in heavy-ion collisions



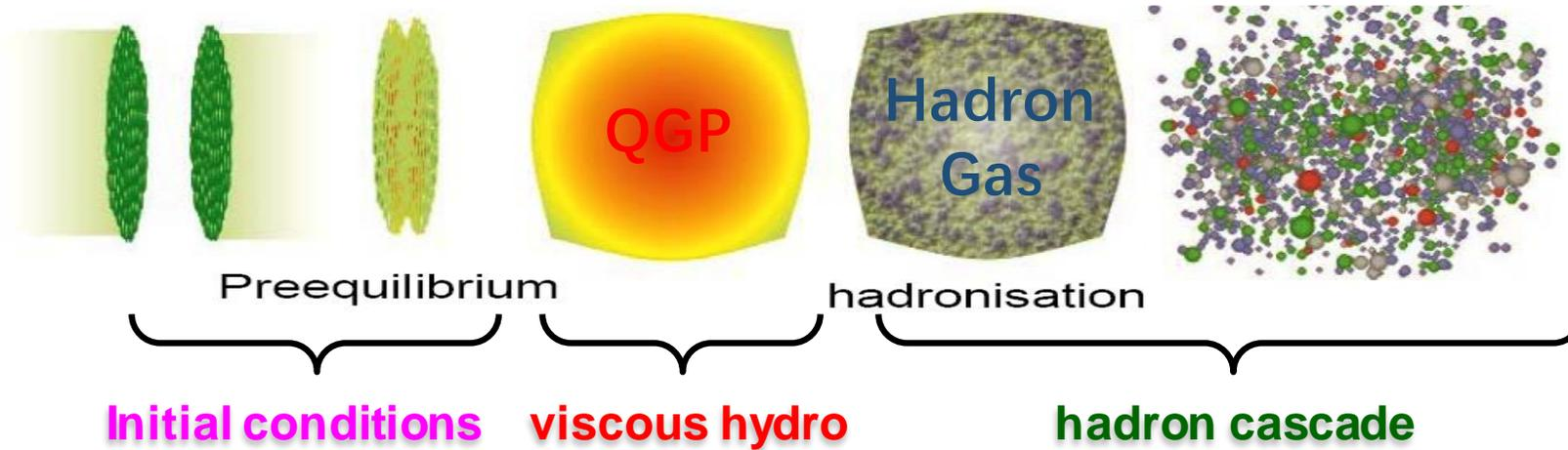
- It has been announced that QGP has been found at RHIC in heavy-ion collisions.

“The Frontiers of Nuclear Science, A Long Range Plan,”
arXiv:0809.3137



Hydrodynamics and Collectivity in A-A collision

Hybrid model



Hydrodynamic evolution:

$$\partial_\mu T^{\mu\nu}(x)=0 \quad \partial_\mu N^\mu(x)=0 \quad \partial \cdot S \geq 0.$$

$$\dot{\Pi} = -\frac{1}{\tau_\Pi} \left[\Pi + \zeta\theta - l_{\Pi q} \nabla_\mu q^\mu + \Pi \zeta T \partial_\mu \left(\frac{\tau_\Pi u^\mu}{2\zeta T} \right) \right],$$

$$\Delta_\nu^\mu \dot{q}^\nu = -\frac{1}{\tau_q} \left[q_\mu + \lambda \frac{nT^2}{e+p} \nabla^\mu \frac{\nu}{T} + l_{q\pi} \nabla_\nu \pi^{\mu\nu} + l_{q\Pi} \nabla^\mu \Pi - \lambda T^2 q^\mu \partial_\mu \left(\frac{\tau_q u^\mu}{2\lambda T^2} \right) \right],$$

$$\Delta^{\mu\alpha} \Delta^{\nu\beta} \dot{\pi}_{\alpha\beta} = -\frac{1}{\tau_\pi} \left[\pi^{\mu\nu} - 2\eta \nabla^{\langle\mu} u^{\nu\rangle} - l_{\pi q} \nabla^{\langle\mu} q^{\nu\rangle} + \pi_{\mu\nu} \eta T \partial_\alpha \left(\frac{\tau_\pi u^\alpha}{2\eta T} \right) \right],$$

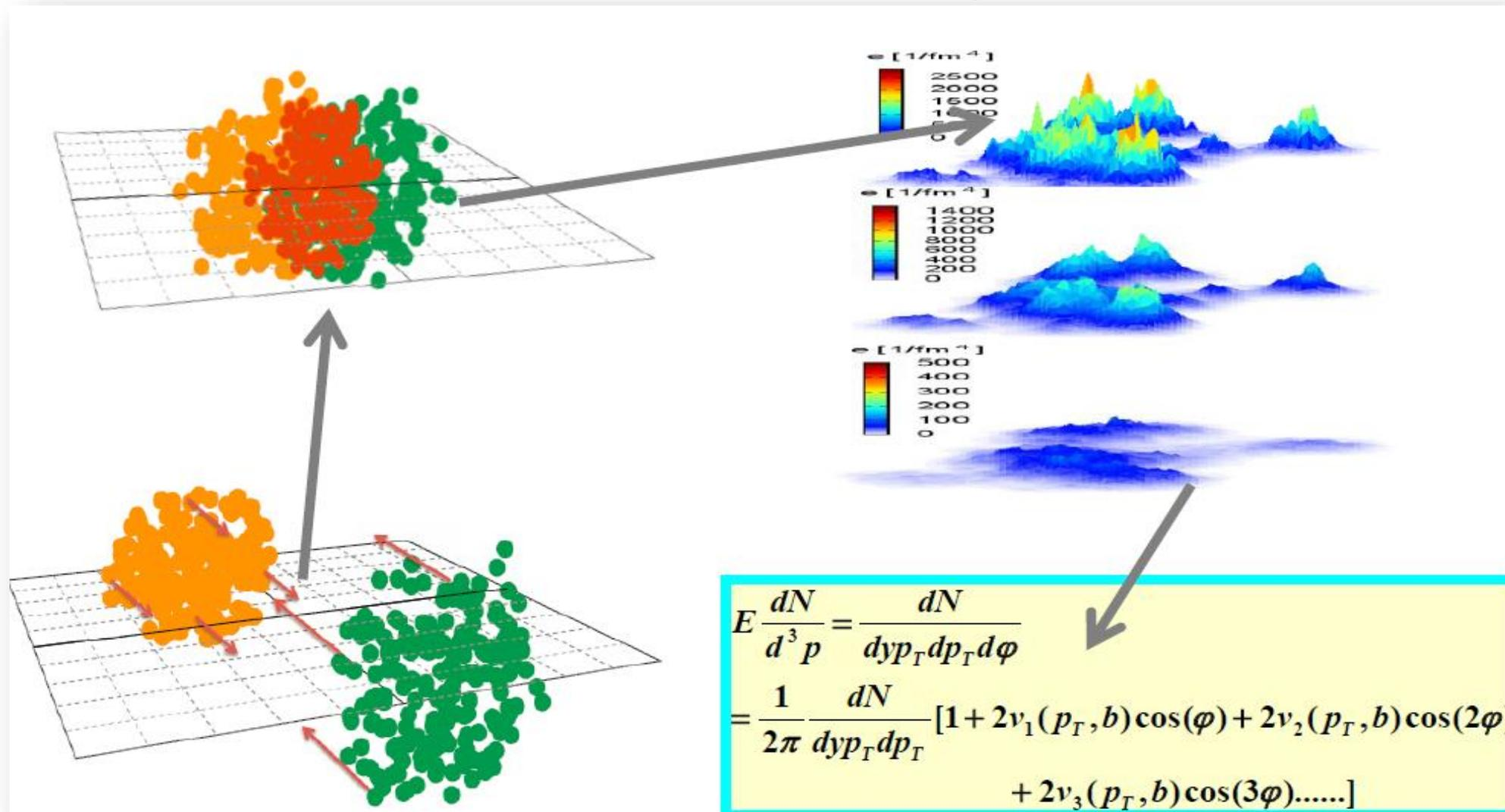
Input:

- 1. EOS**
- 2. Initial conditions**

C.Shen, Z.Qiu, H.Song, J.Bernhard, S.Bass and U.Heinz *Comput. Phys. Commun*,199,61 (2016).

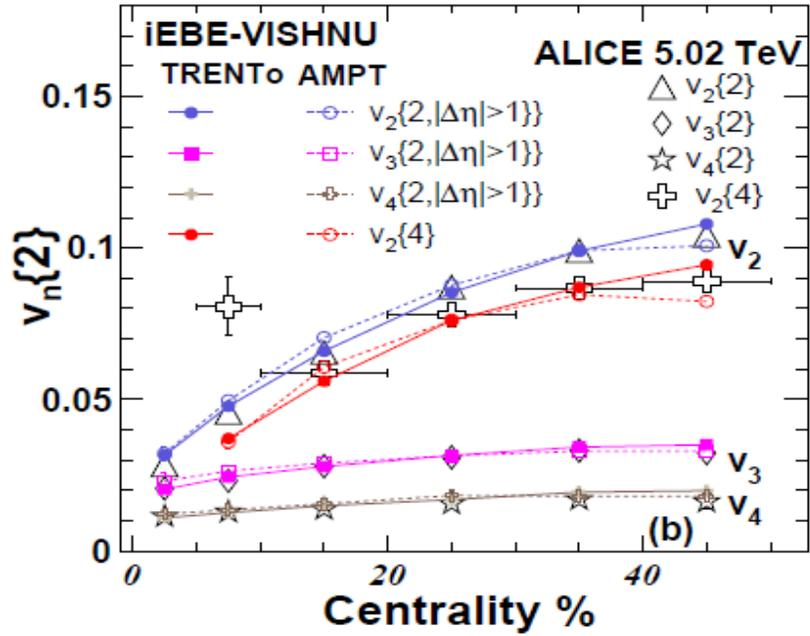
H.Song, S.A.Bass and U.Heinz, *Phys. Rev. C* 83, 024912 (2011).

Fluctuations and Correlations in heavy-ion collisions

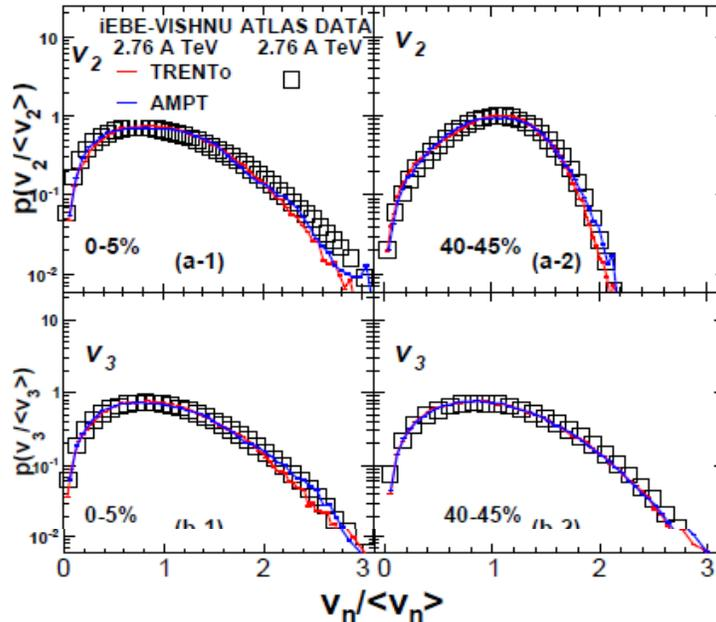


- In heavy-ion collisions, hydrodynamics transform the initial state fluctuations to final state correlations.

Pb+Pb 5.02 A TeV



Pb+Pb 2.76 A TeV

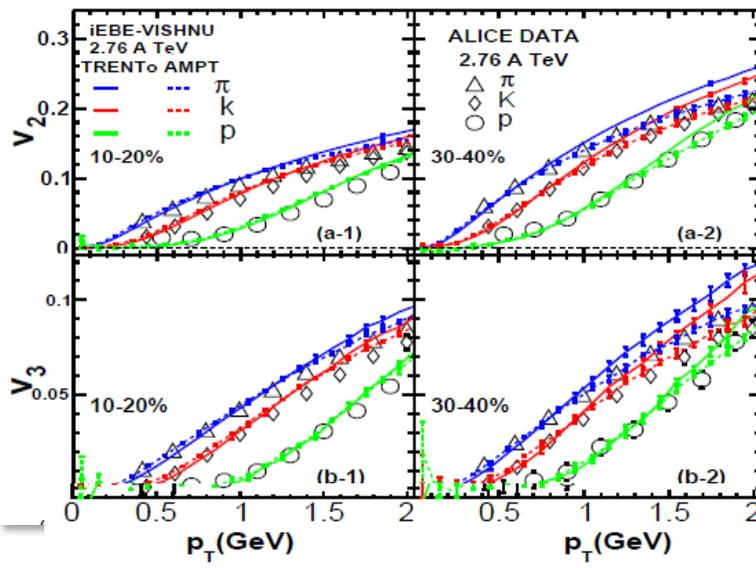


Other flow observables

- Event-plane correlations
- Non-linear response coefficients
- Decorrelations at p_T direction.
- ...

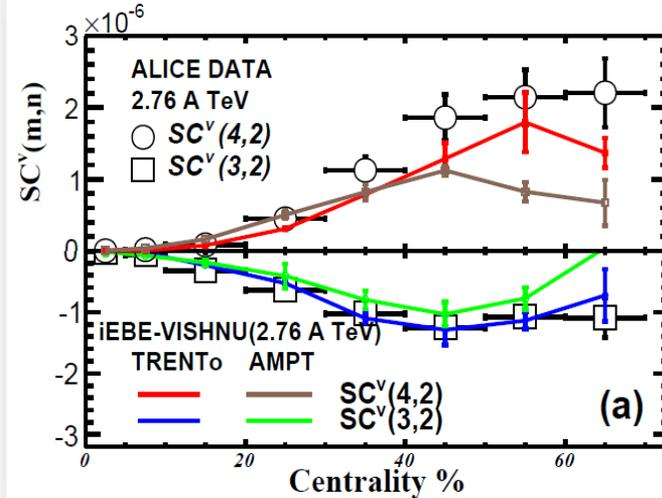
W. Zhao, H. j. Xu and H. Song, Eur. Phys. J. C 77, no. 9, 645 (2017).

Pb+Pb 2.76 A TeV



$$SC^V(m, n) = \langle v_m^2 v_n^2 \rangle - \langle v_m^2 \rangle \langle v_n^2 \rangle$$

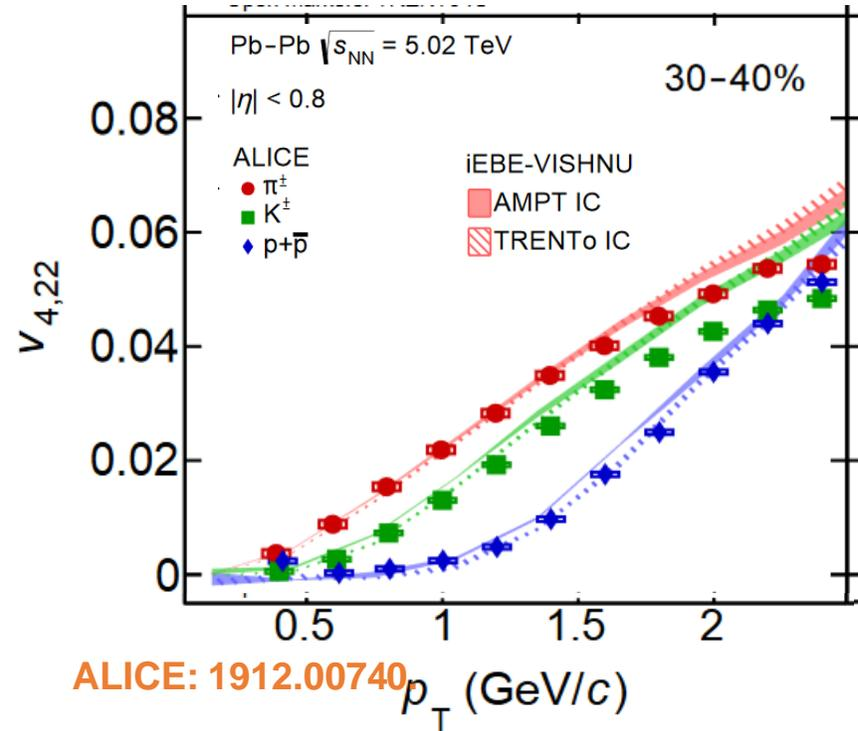
Pb+Pb 2.76 A TeV



- Hydrodynamic model does a great job in describing the hydrodynamic evolutions of heavy-ion collisions.

The predictions from hydrodynamics

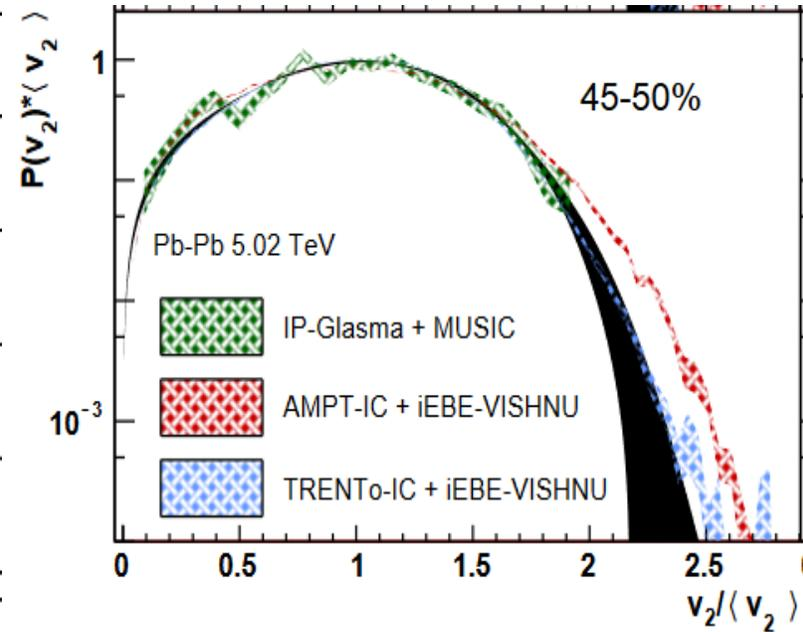
- Non-linear flow modes



$$V_4 = V_4^L + V_4^{NL} = V_4^L + \chi_{4,22}(V_2)^2,$$

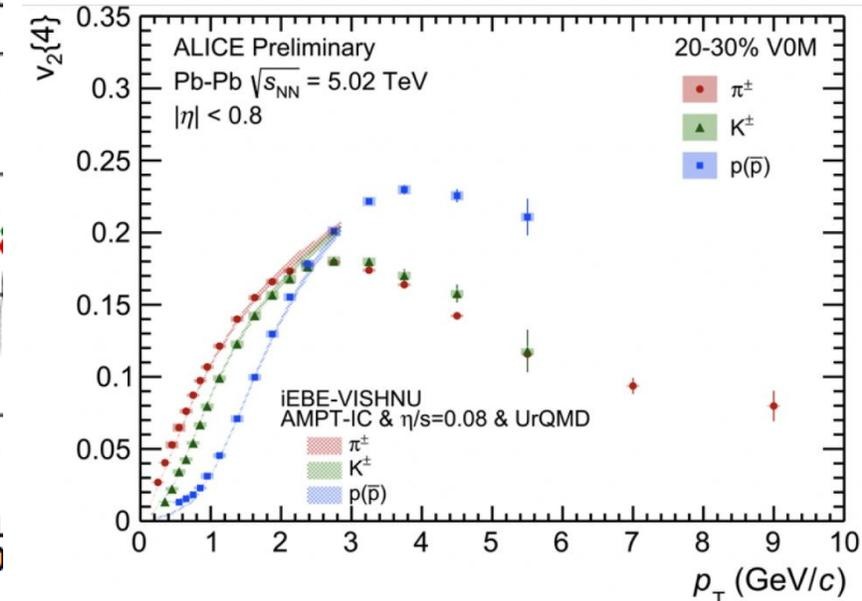
- In heavy-ion collisions, hydrodynamics has the strong predictive power for the collective flow observables at low p_T range.
- It can constrain the initial models and extract the QGP transport coefficients from various bulk observables.

- Flow distributions



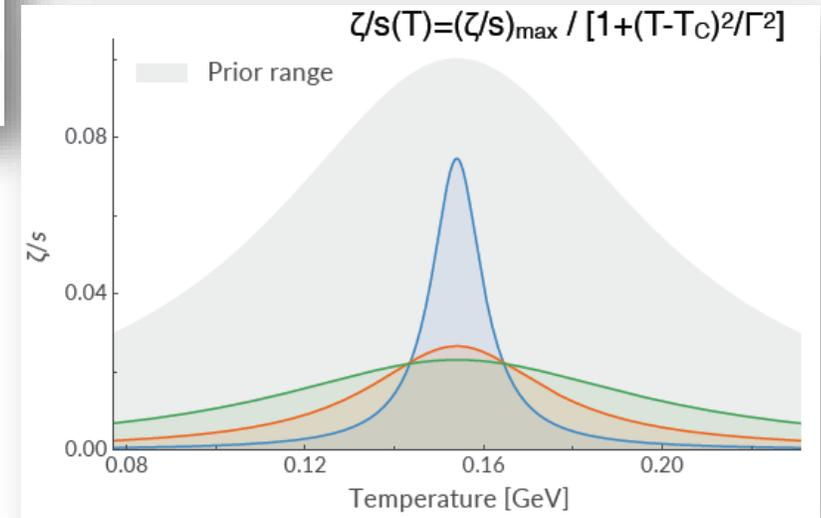
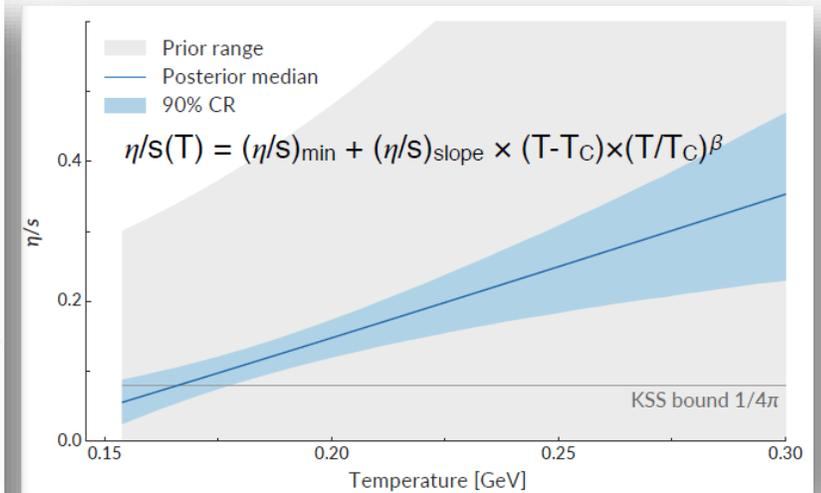
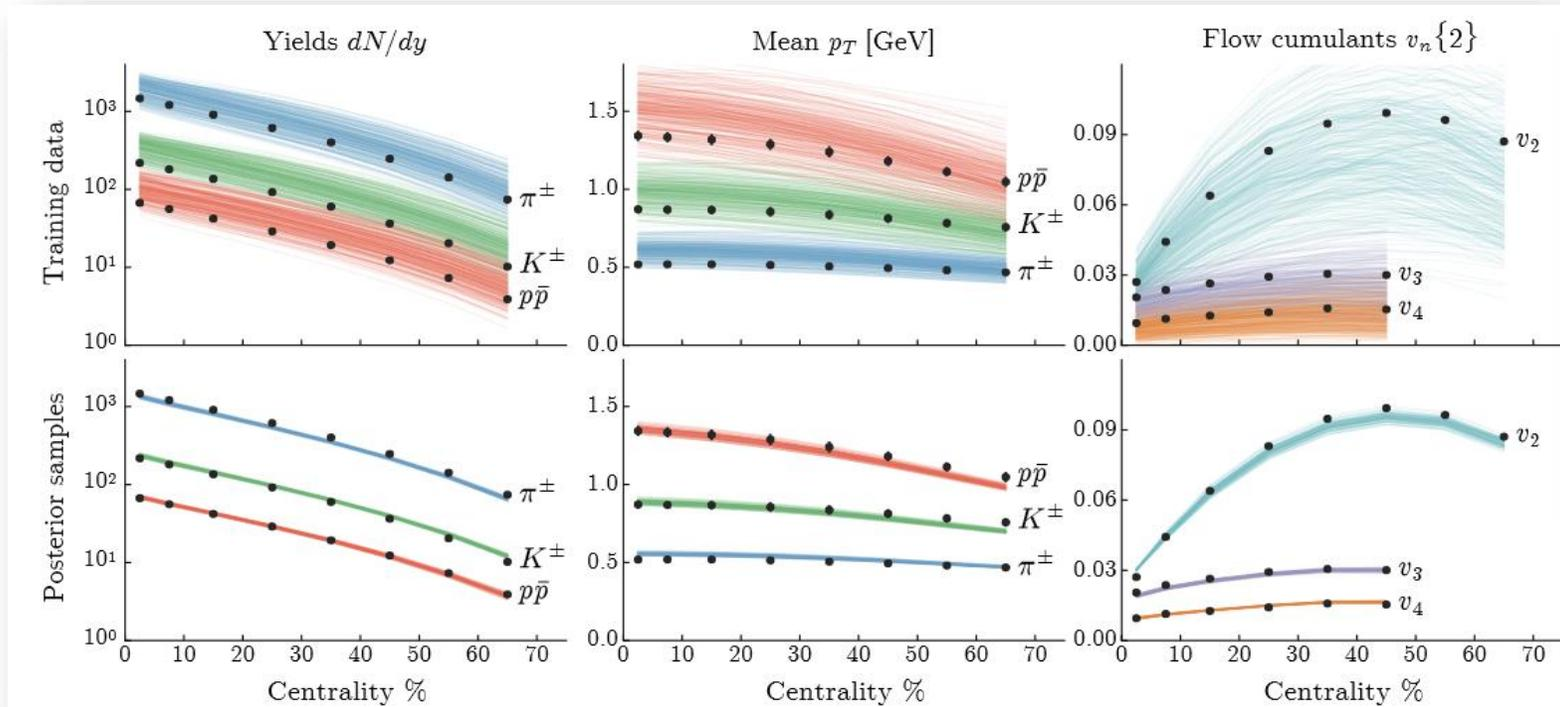
ALICE: JHEP 1807,103(2018)

- $v_2\{4\}(p_T)$ of π , K and P.



Ya Zhu Quark Matter 2019 Wuhan

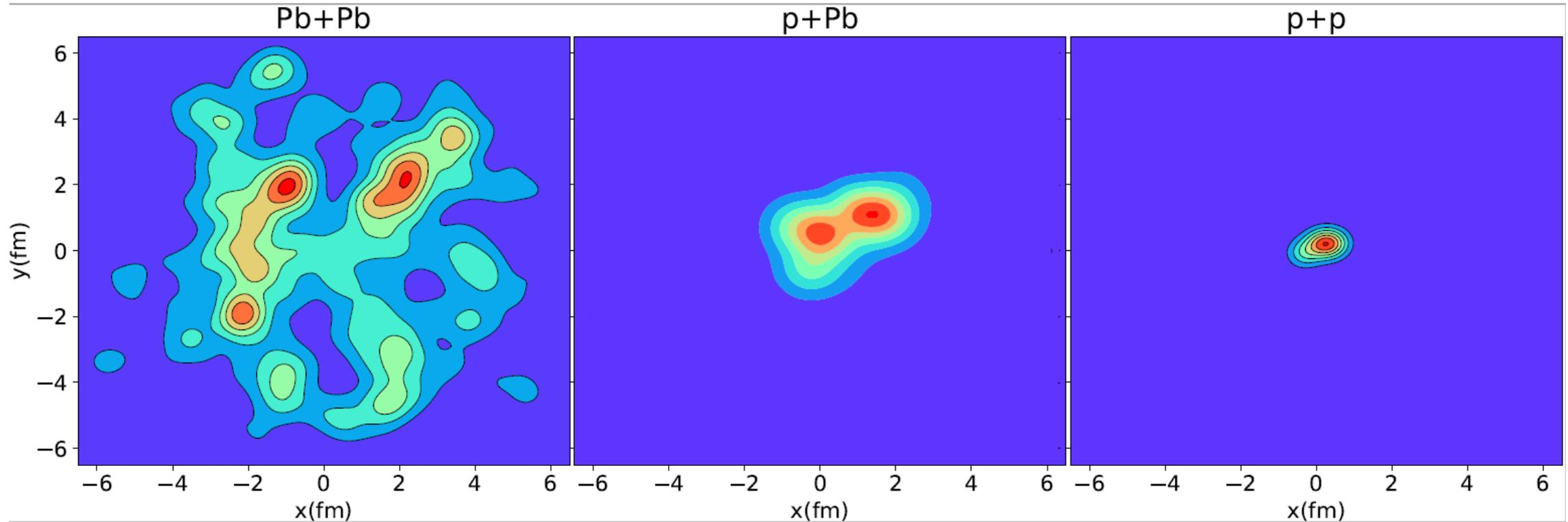
Extract the QGP transport coefficients by Bayesian global fitting



J. Bernhard, et.al. PRC 94, 024907 (2016).
Nature Phys.15 (2019) 11, 1113.

- Using Bayesian global fitting within the framework of TRENTo+iEBE-VISHNU to extract the QGP specific shear viscosity and bulk viscosity.
- LHC of Pb+Pb collisions flow data show good constraining power on the temperature dependence of QGP shear and bulk viscosity.
- The extracted η/s is close to the KSS bound of $1/4\pi$.

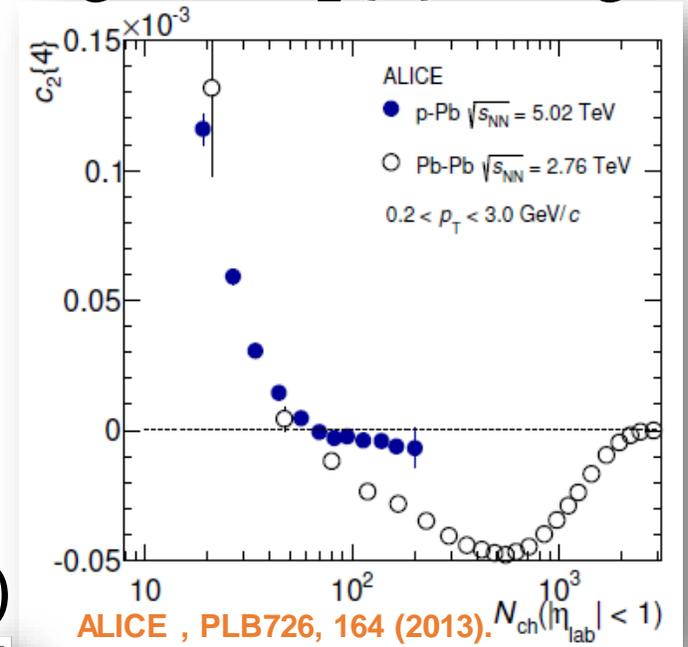
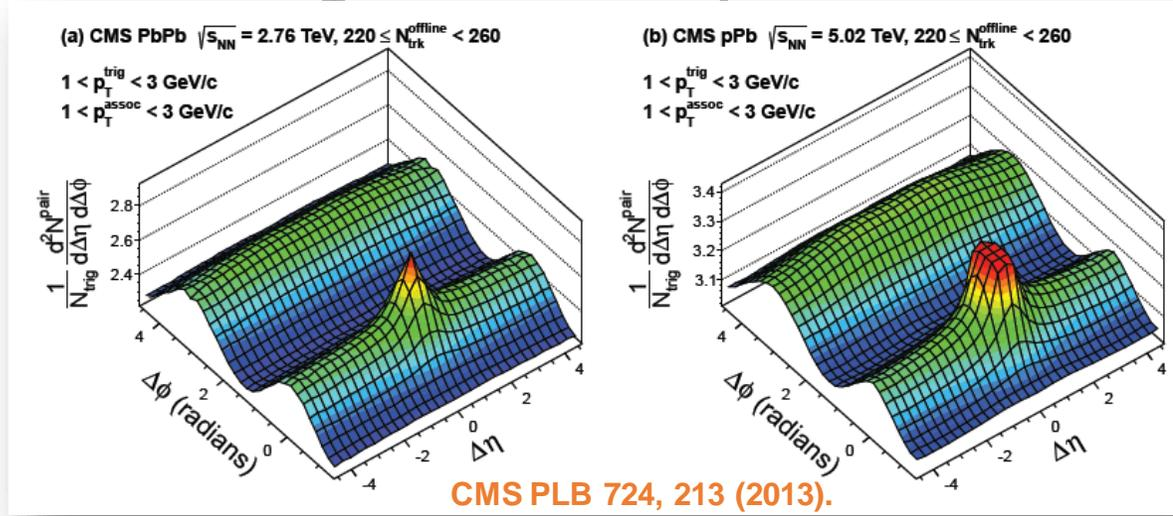
Collectivity & QGP signatures in small systems



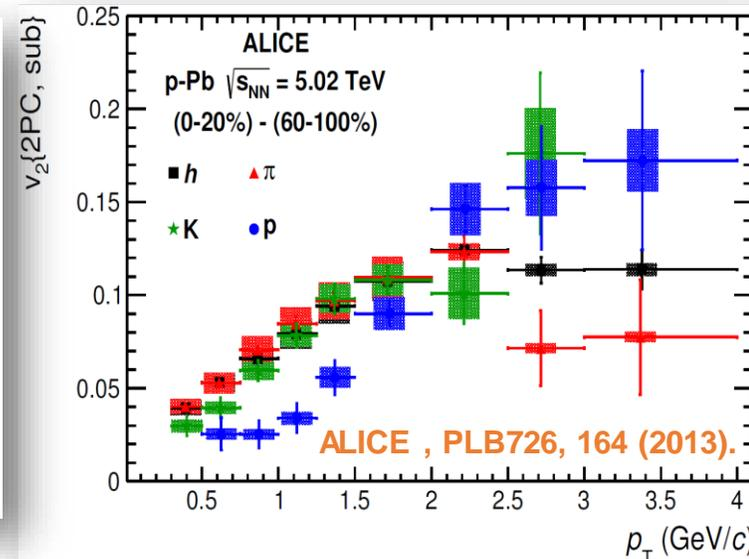
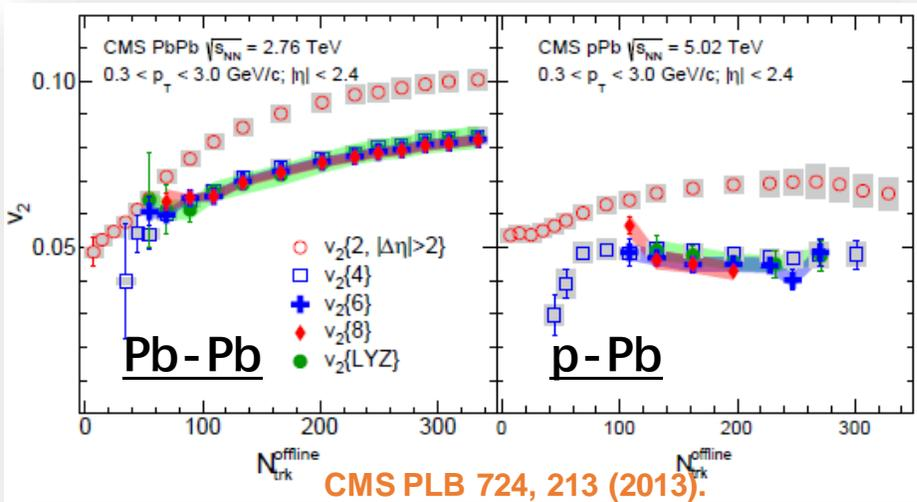
Plot with TRENTo initial condition.

Collective flow? experimental observables in p-Pb collisions

- Similar "ridge" structure p+Pb and Pb + Pb system
- Negative $c_2\{4\}$ at high mult.

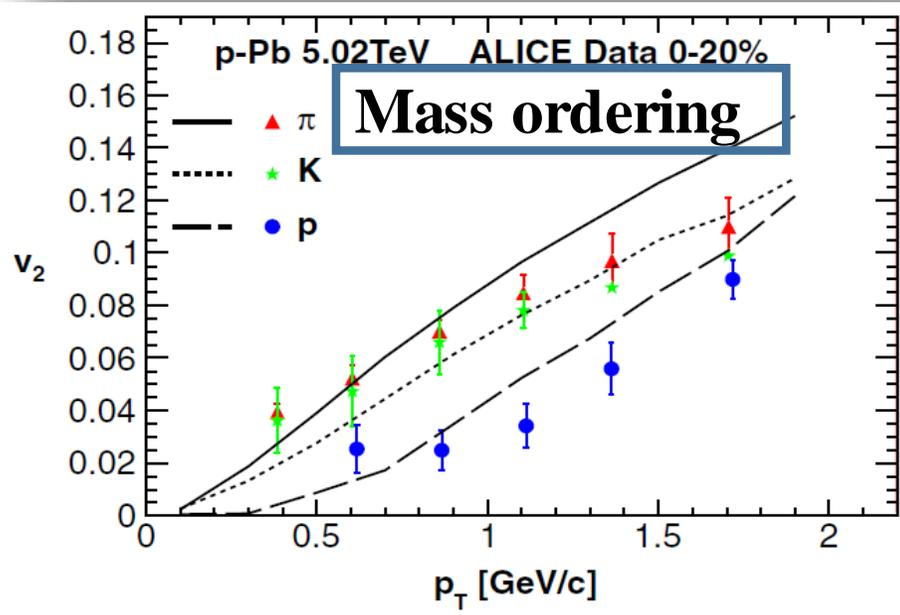
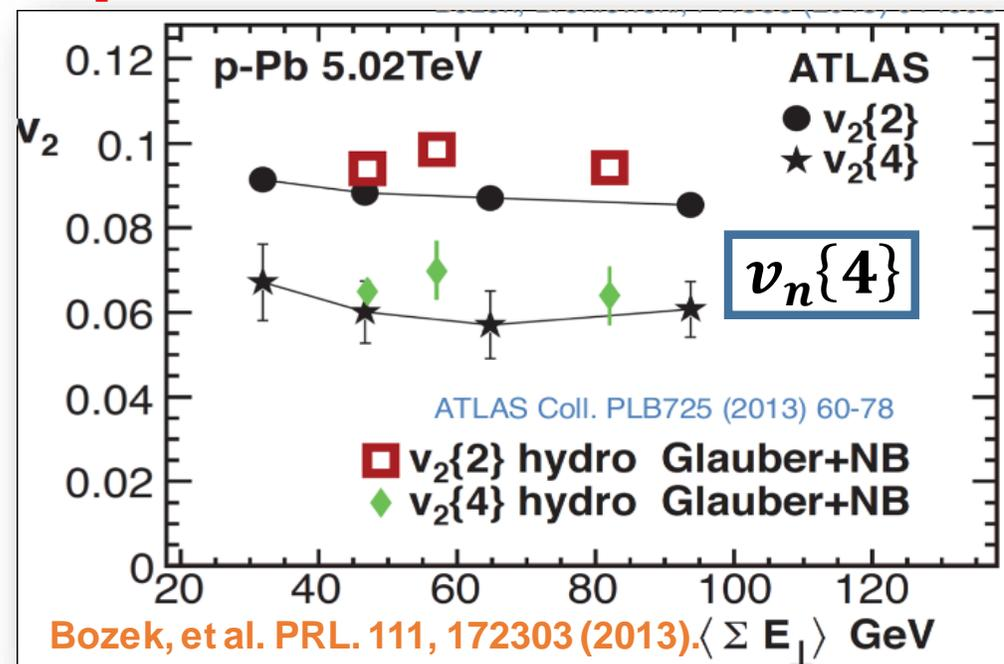
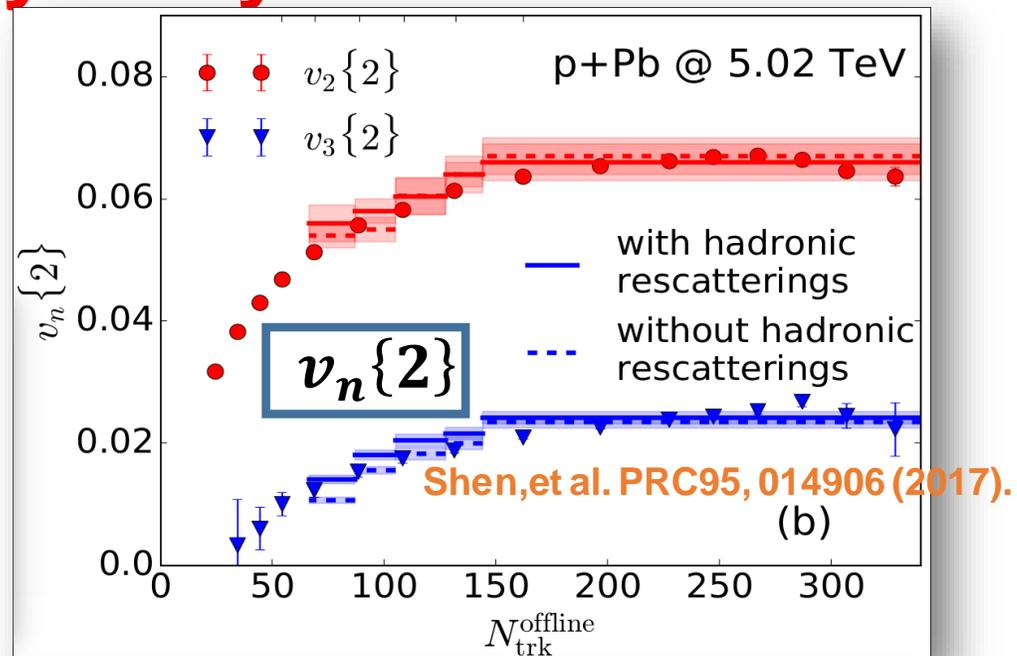


- Multi-particle correlation
- Mass ordering of $v_2(p_T)$



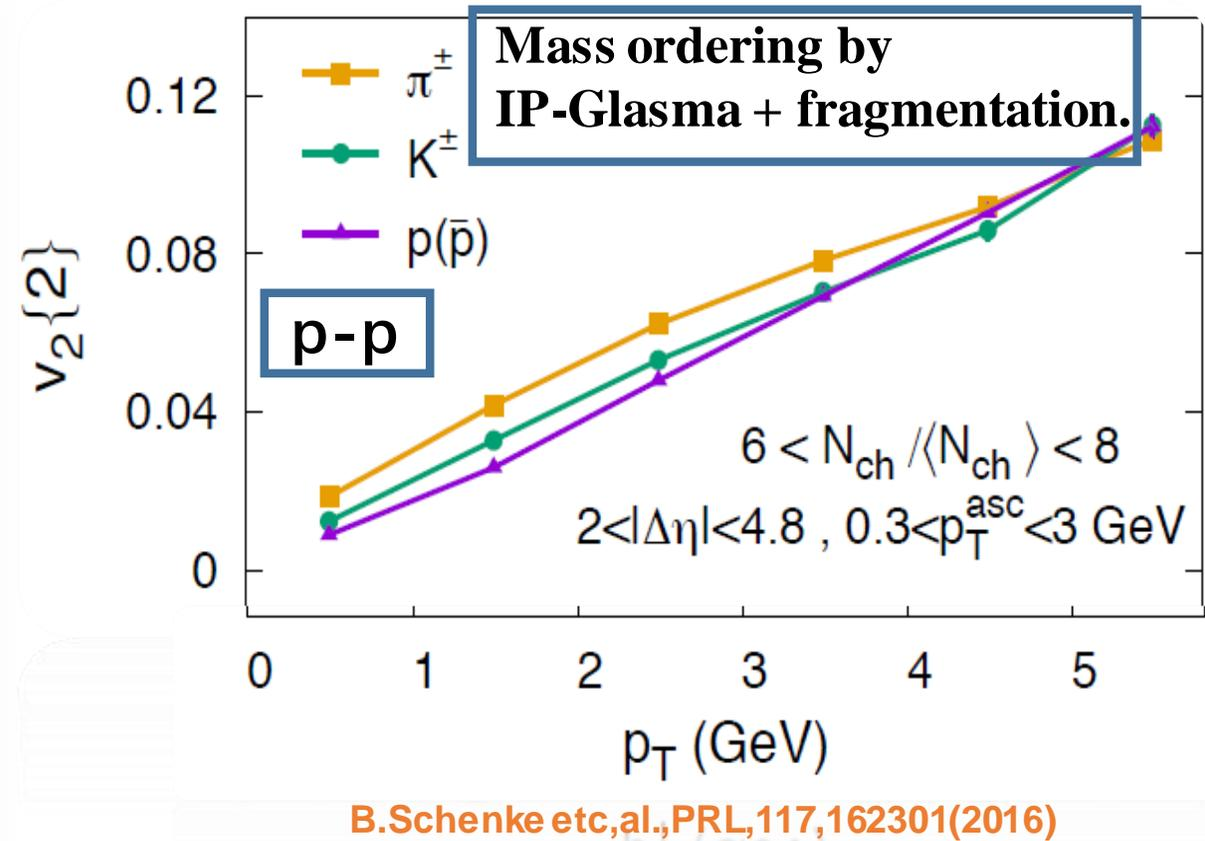
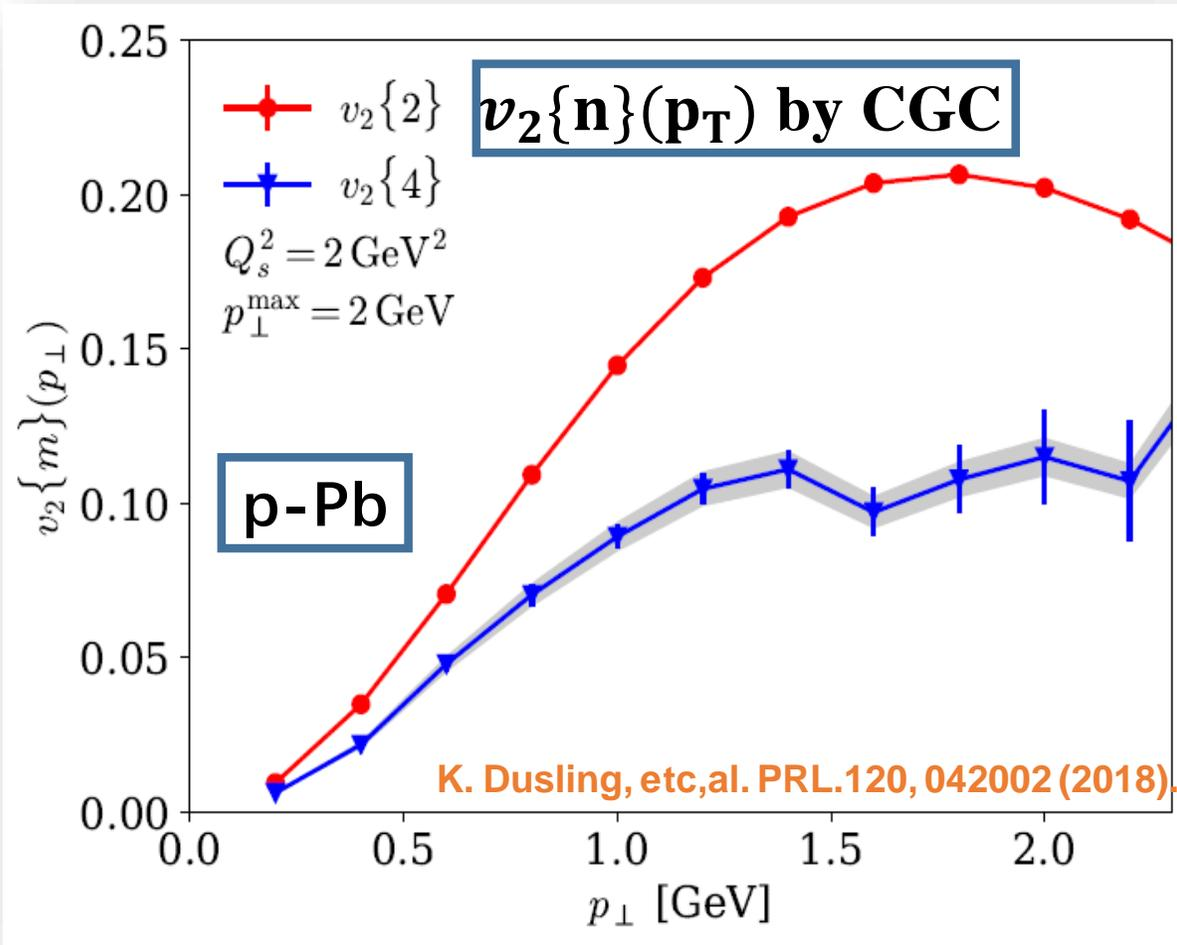
- The indication of collectivity in high-multiplicity p-Pb collisions.

Hydrodynamic simulations in p-Pb



- Hydrodynamics can well reproduce “collectivity” features in p-Pb system.

Initial states correlations in small system



- Without QGP effects, initial state correlation also describe many “collective” features, such as multi-particle correlations and mass ordering in small systems

Initial state or Final state effects?

Initial state effects:

– Various Models interpolations

- K. Dusling and R. Venugopalan, PRL 2012, PRD2013, NPA 2014.
- A. Dumitru and A. V. Giannini, NPA 2015, A. Dumitru and V. Skokov PRD2015.
- B. Schenke, S. Schlichting, P. Tribedy, and R. Venugopalan, PRL2016.
- K. Dusling et al, Phys. Rev. Lett 120 042002 (2018)..
- C. Zhang, et al Phys. Rev. Lett. 122, no. 17, 172302 (2019).

... ..

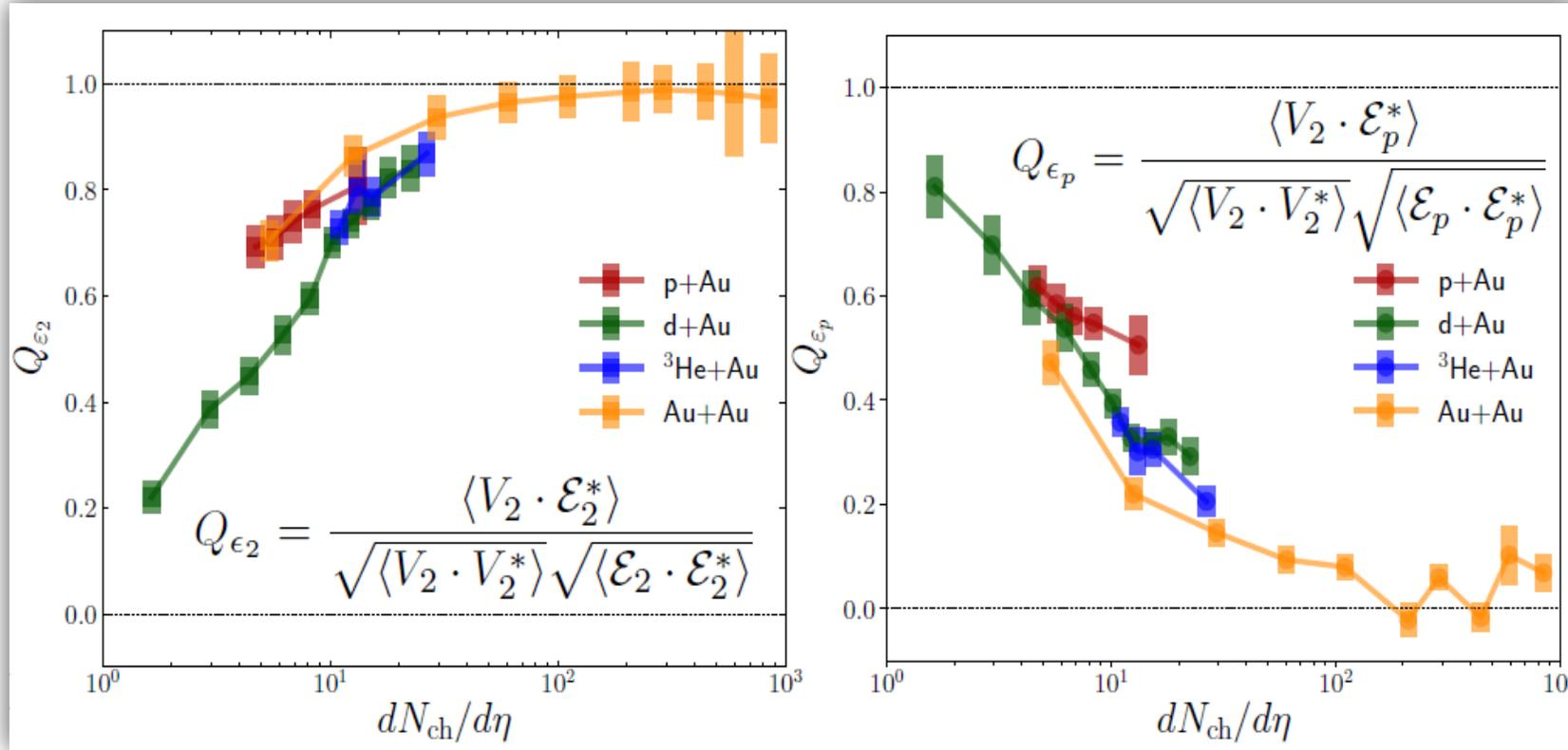
Final state effects:

- P. Bozek, W. Broniowski, G. Torrieri, PRL2013.
- K. Werner, et. Al., PRL2014.
- G.-Y. Qin, B. Muller. PRC2014.
- A. Bzdak and G. L. Ma, PRL 113, 25, 252301 (2014).
- P. Bozek, A. Bzdak, and G.-L. Ma, PLB2015.
- P. Romatschke, Eur.Phys.J. C77 21(2017).
- W. Zhao, Y. Zhou, H. Xu, W. Deng and H. Song, Phys. Lett. B 780, 495 (2018).

... ..

Hybrid model with initial and final states correlations

IP-Glasma +MUSIC+UrQMD



- Initial state geometry vector

$$\epsilon_2 e^{i2\Psi_2^{\text{PP}}} = -\frac{\int d^2\mathbf{r} r^2 s(r, \phi) e^{i2\phi}}{\int d^2\mathbf{r} r^2 s(r, \phi)}$$

- Initial state momentum anisotropy

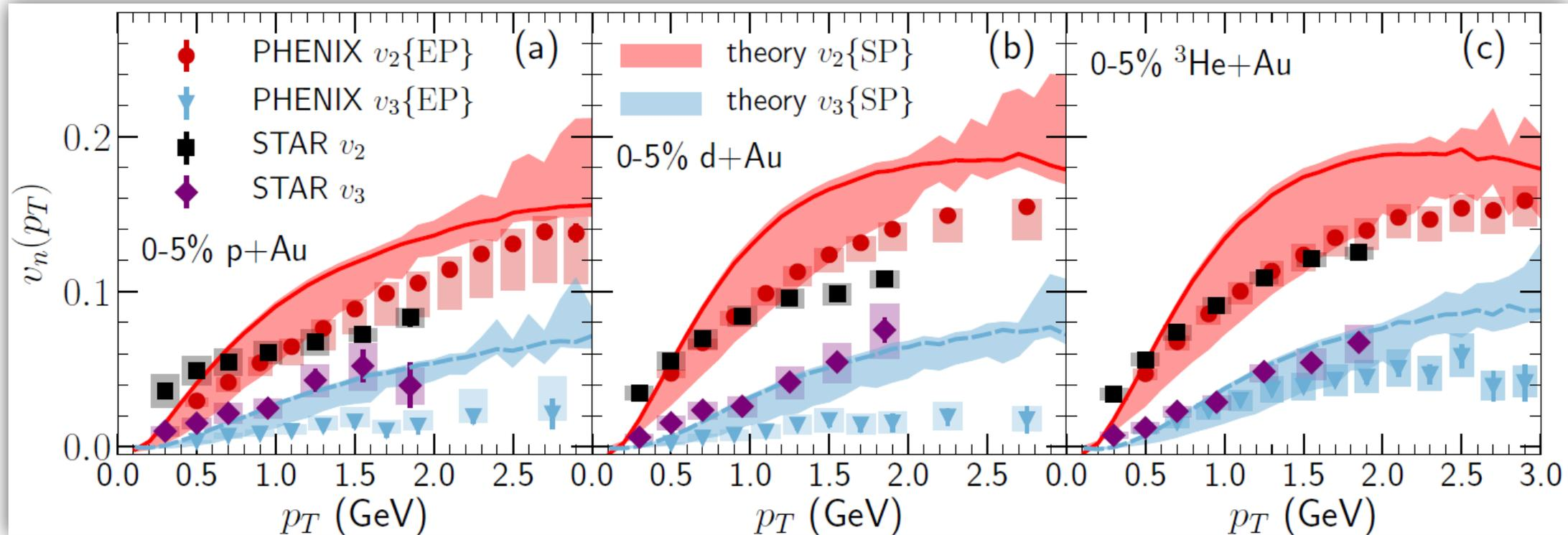
$$\vec{\mathcal{E}}_p = \epsilon_p e^{2i\psi_2^p} = \frac{\langle T^{xx} - T^{yy} \rangle + i\langle 2T^{xy} \rangle}{\langle T^{xx} + T^{yy} \rangle}$$

B.Schenke, C. Shen and P.Triedy,PLB,803,135322(2020).

B.Schenke QM 2019.

- Below $dN_{ch}/d\eta \sim 10$, the initial momentum anisotropy contributes strongly to the final charged hadron elliptic anisotropy;
- Above $dN_{ch}/d\eta \sim 100$, everything is geometry driven.

System size scan of v_n at RHIC



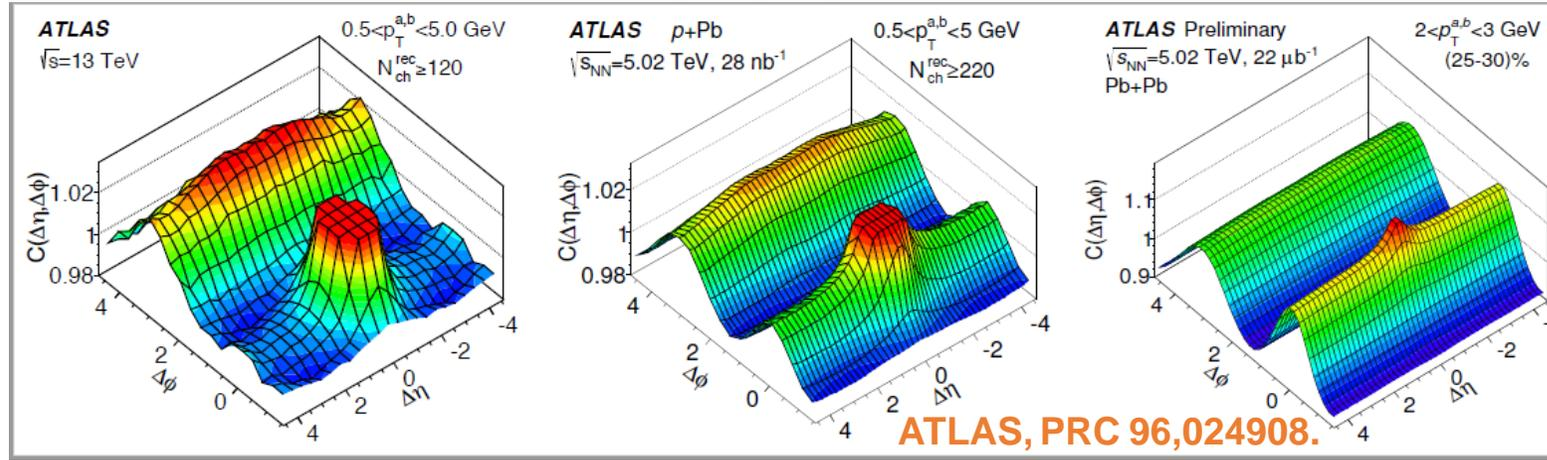
IP-Glasma+MUSIC+UrQMD calculations: B.Schenke, C. Shen and P.Tribedy, PLB, 803, 135322 (2020). B.Schenke QM 2019.
STAR data: Quark Matter 2019; PHENIX data: Nature Phys. 15, 214 (2019).

- The observed $v_2(p_T)$ is similar between STAR and PHENIX for all systems.
- The observed $v_3(p_T)$ from STAR is much larger than that from PHENIX, especially for p-Au and d-Au collisions.
- The hydro calculations with nucleonic substructure is consistent with the STAR data.

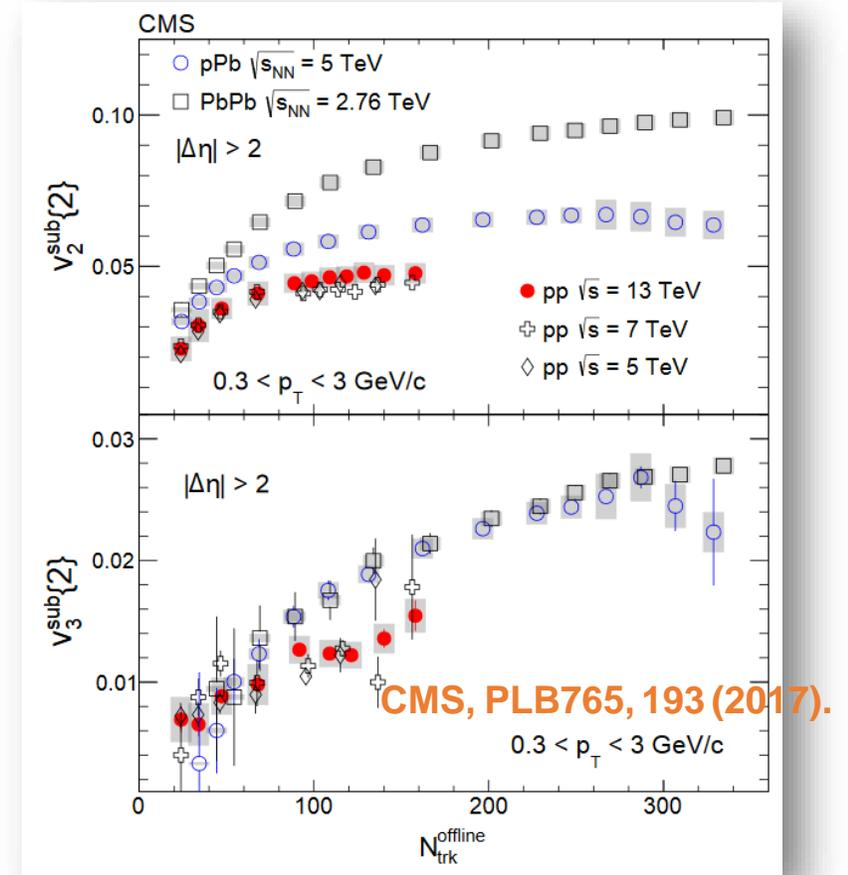
Collectivity in p-p Collisions at 13 TeV

2-particle correlations in p-p collisions

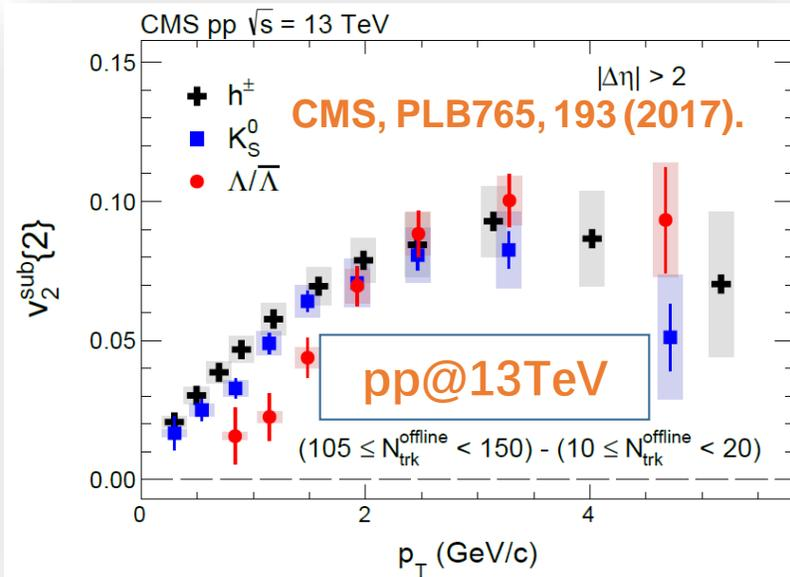
- “ridge” structures in p+p, p+Pb and Pb + Pb



- $v_2\{2\}$ and $v_3\{2\}$

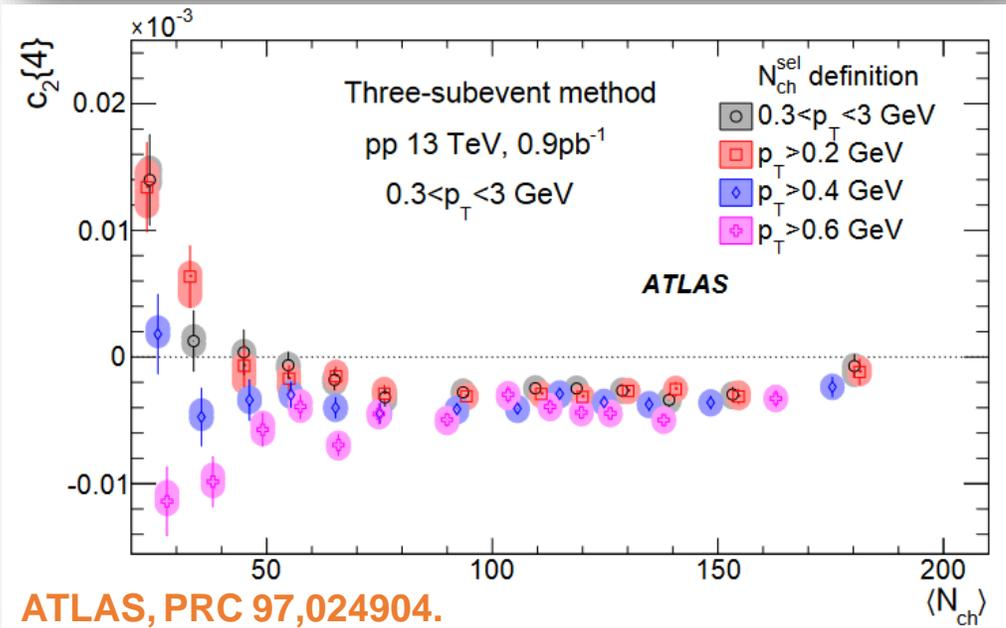
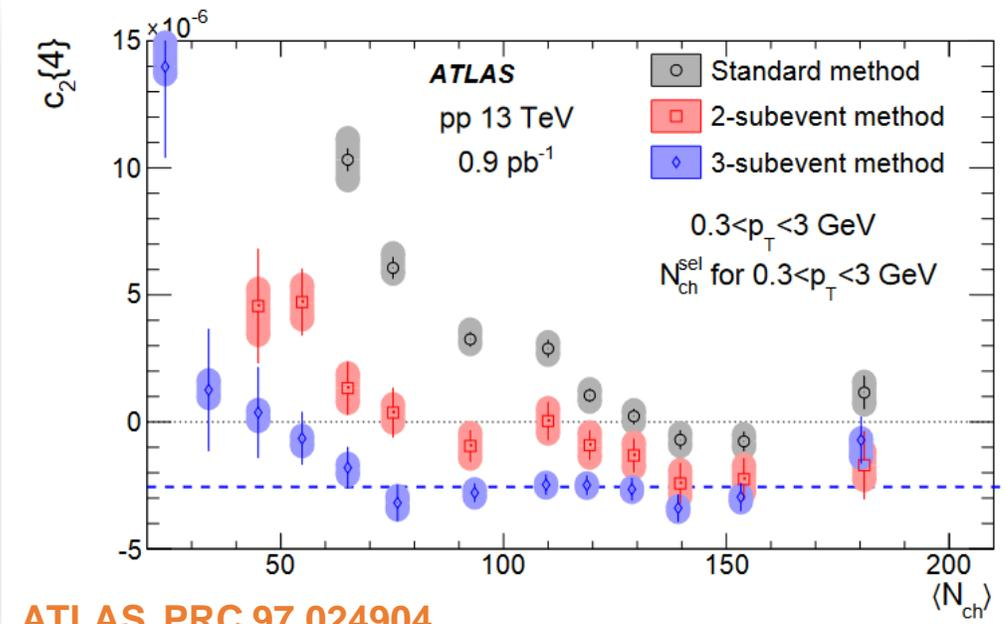


- Mass ordering of $v_2(p_T)$



- Similar double ridge structure, but with smaller magnitudes in p-p collisions.
- Observed the $v_2\{2\}$ and $v_3\{3\}$ in p-p collisions.
- Clear mass ordering of v_2 in high multiplicity p-p collisions.

4-particle correlations in p-p collisions

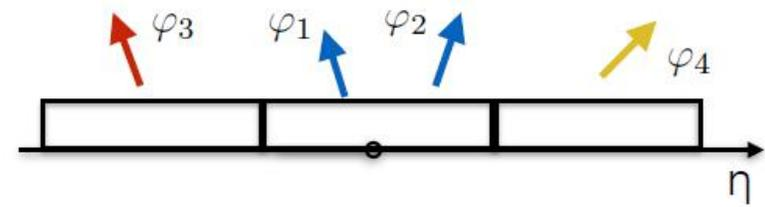


$$\langle\langle 4 \rangle\rangle_{3\text{sub}} = \langle\langle \cos n(\varphi_1 + \varphi_2 - \varphi_3 - \varphi_4) \rangle\rangle$$

$$\langle\langle 2 \rangle\rangle_{3\text{sub}}^2 = \langle\langle \cos n(\varphi_1 - \varphi_3) \rangle\rangle \langle\langle \cos n(\varphi_2 - \varphi_4) \rangle\rangle$$

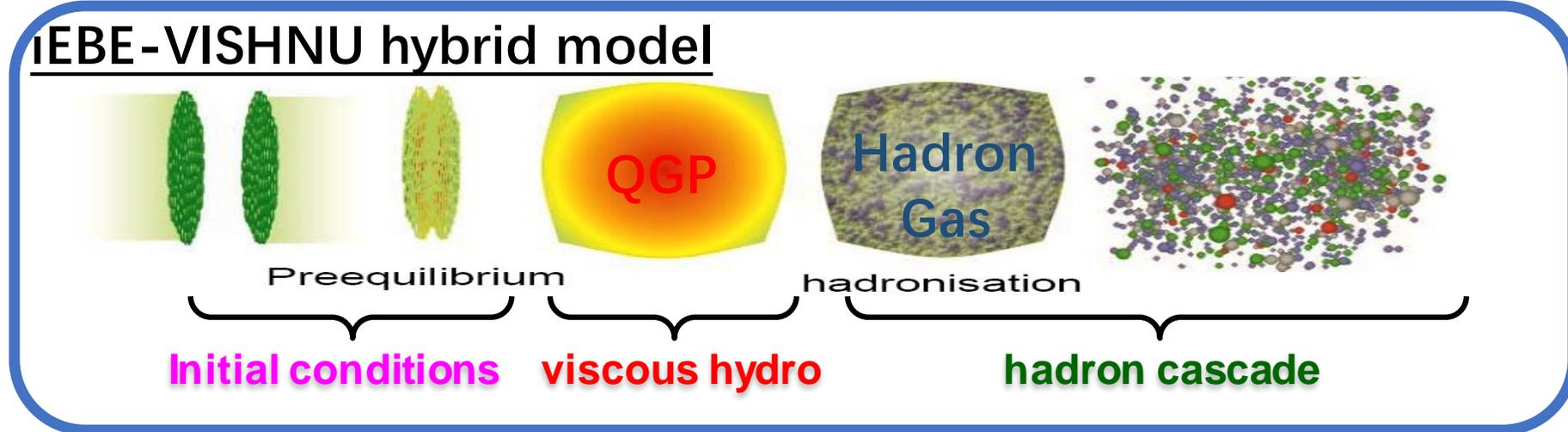
$$\langle\langle 2 \rangle\rangle_{3\text{sub}}^2 = \langle\langle \cos n(\varphi_1 - \varphi_4) \rangle\rangle \langle\langle \cos n(\varphi_2 - \varphi_3) \rangle\rangle$$

$$c_n\{4\}_{3\text{sub}} = \langle\langle 4 \rangle\rangle_{3\text{sub}} - 2 \cdot \langle\langle 2 \rangle\rangle_{3\text{sub}}^2$$



- The three-subevent can effectively suppress the non-flow and get the negative $c_2\{4\}$ in p-p collisions.
- The $c_2\{4\}$ obtained by three-subevent weakly depend on N_{ch}^{sel} in high multiplicity in p-p collisions.

Hydrodynamic Collectivity in p+p collisions at 13 TeV



HIJING initial condition

X. N.Wang and M.Gyulassy, *Phys. Rev. D* 44, 3501 (1991).

W. Zhao, Y. Zhou, H. Xu, W. Deng and H. Song, *Phys. Lett. B* 780, 495 (2018).

- produced jets pairs & excited nucleus → independent strings
- strings break into partons → form hot spots for succeeding hydro.

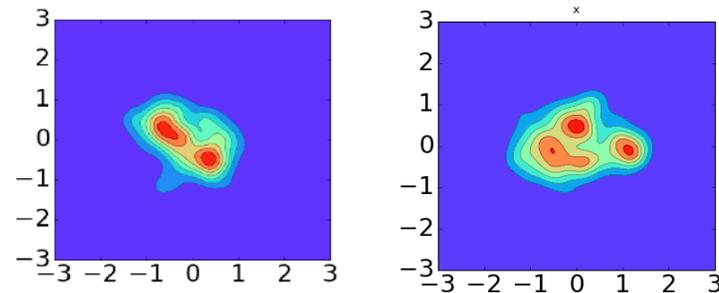
1) The center positions of strings (x_c, y_c) are sampled by Saxon-Woods distribution

2) positions of partons within the strings are sampled by

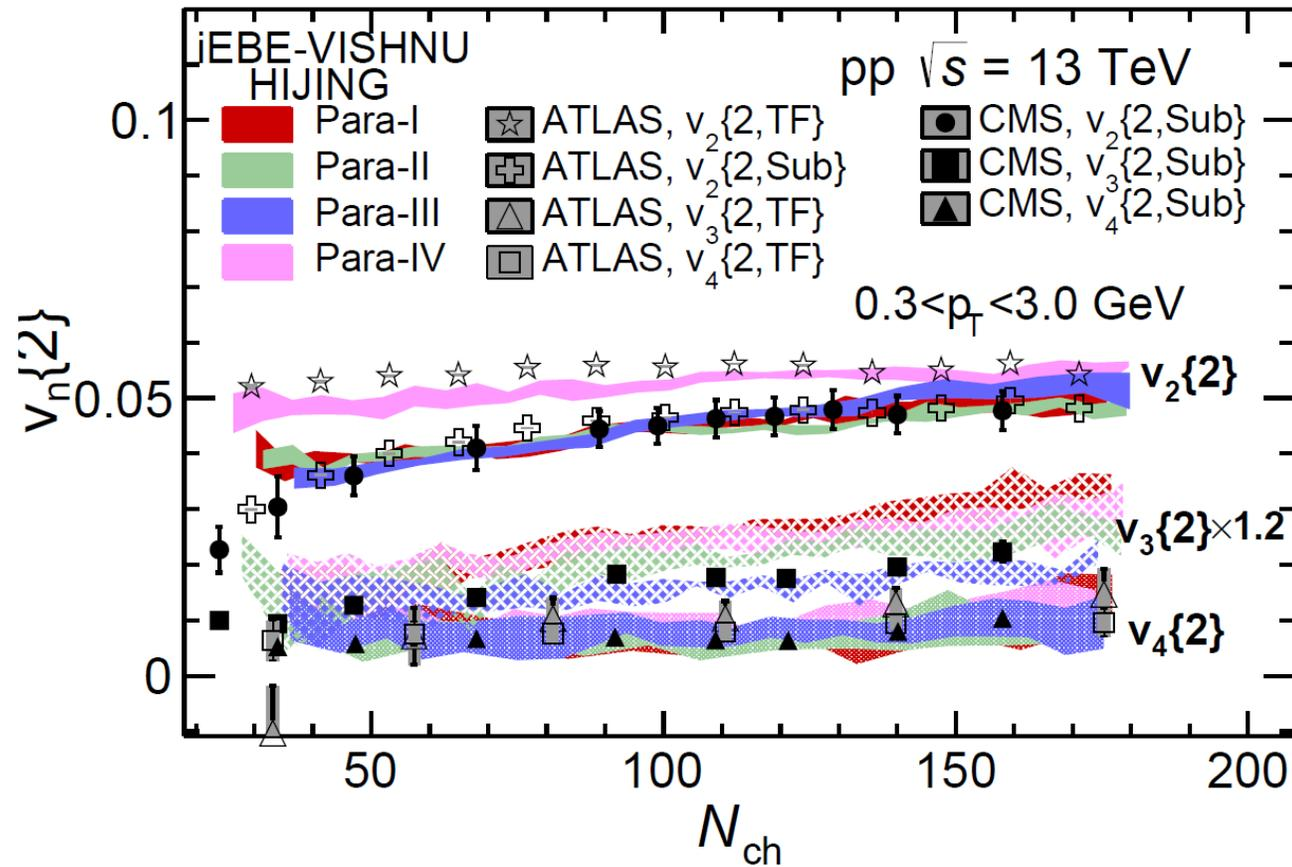
$$\exp\left(-\frac{(x-x_c)^2+(y-y_c)^2}{2\sigma_R^2}\right)$$

3) Energy decompositions of individual partons with a Gaussian smearing:

$$\epsilon = K \sum_i \frac{E_i^*}{2\pi\sigma^2\tau_0\Delta\eta_s} \exp\left(-\frac{(x-x_i)^2+(y-y_i)^2}{2\sigma^2}\right),$$



2-particle correlation in p-p collisions



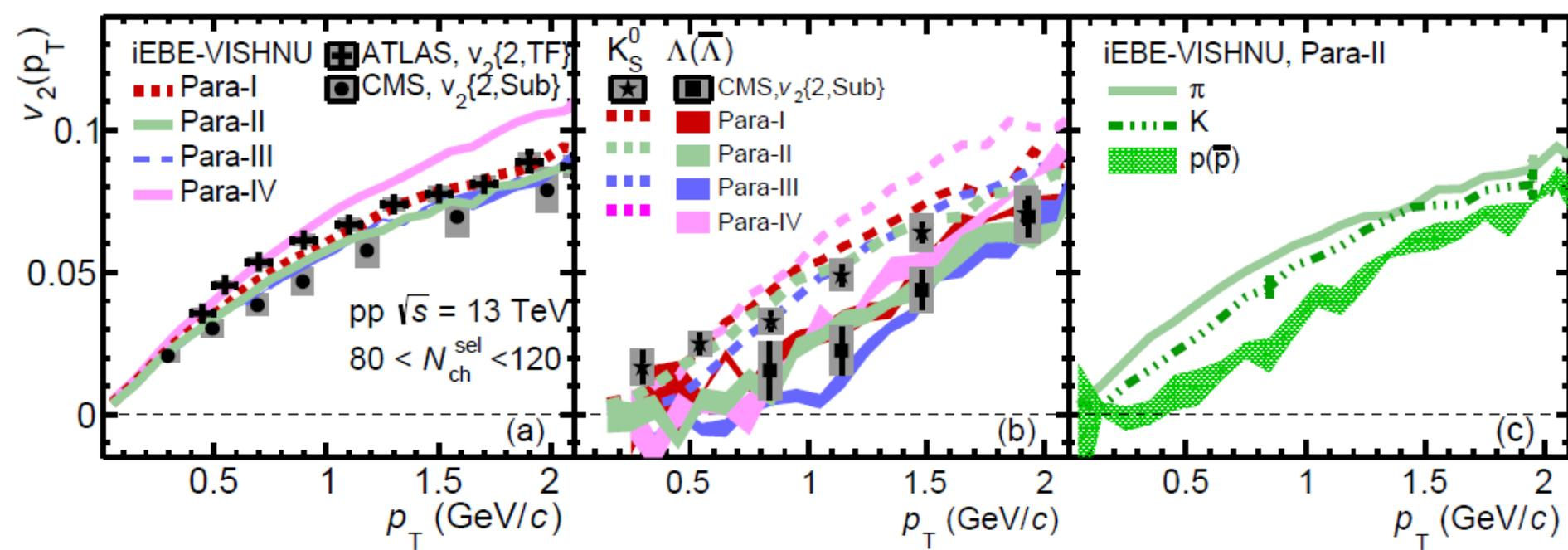
$$v_n\{2\} = \sqrt{\langle v_n^2 \rangle} = \sqrt{\langle v_n \rangle^2 + \sigma_{v_n}^2}$$

$$(v_n = \langle v_n \rangle + \sigma_{v_n})$$

W. Zhao, Y. Zhou, H. Xu, W. Deng and H. Song,
 Phys. Lett. B 780, 495 (2018)

- iEBE-VISHNU + HIJING, use three set-ups to fit CMS $v_2\{2\}$, one to fit ATLAS $v_2\{2\}$.
- In general, iEBE-VISHNU + HIJING can describe the $v_2\{2\}$ and $v_4\{2\}$ from ATLAS and CMS. But iEBE-VISHNU + HIJING tend to overestimate the observed $v_3\{2\}$.
- $v_2\{2\}$ calculated by iEBE-VISHNU + HIJING increase slowly as a function of multiplicity.

Differential elliptic flow

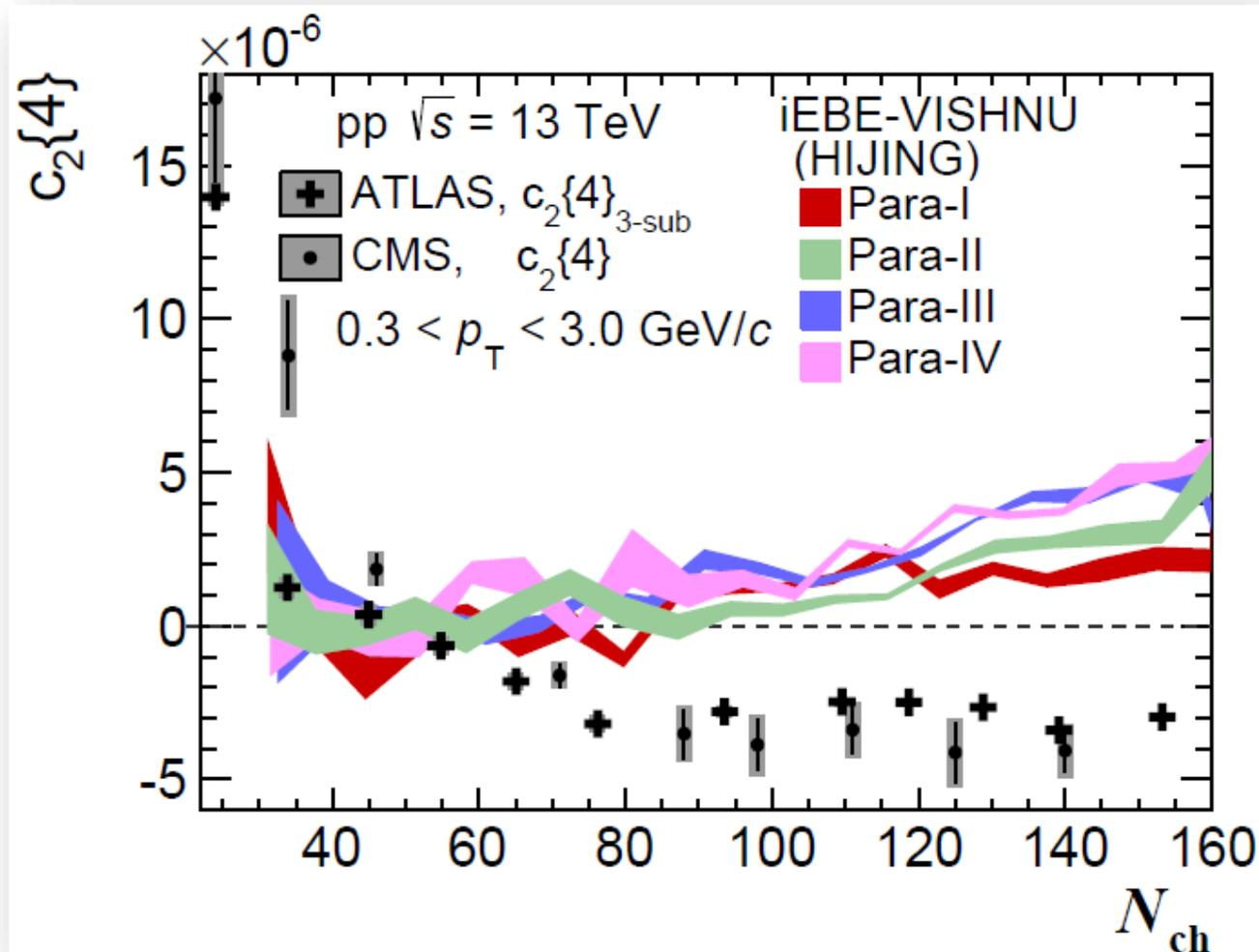


$$v_n\{2\} = \sqrt{\langle v_n^2 \rangle} = \sqrt{\langle v_n \rangle^2 + \sigma_{v_n}^2}, \quad (v_n = \langle v_n \rangle + \sigma_{v_n})$$

W. Zhao, Y. Zhou, H. Xu, W. Deng and H. Song,
Phys. Lett. B 780, 495 (2018)

- In general, iEBE-VISHNU + HIJING can describe the $v_2(p_T)$ from ATLAS and CMS well.
- Hydrodynamics can well reproduce the mass ordering of $v_2(p_T)$ among K_S^0 and Λ as observed in experimental data in high multiplicity p-p collisions.

4-particle correlation by hydrodynamic simulations in p-p



$$c_2\{4\} = -2\langle v_2^2 \rangle^2 + \langle v_2^4 \rangle$$

$$= -\langle v_2 \rangle^4 + 2\sigma_{v_2}^2 \langle v_2^2 \rangle^2 + \sigma_{v_2}^2$$

$$(v_2 = \langle v_2 \rangle + \sigma_{v_2})$$

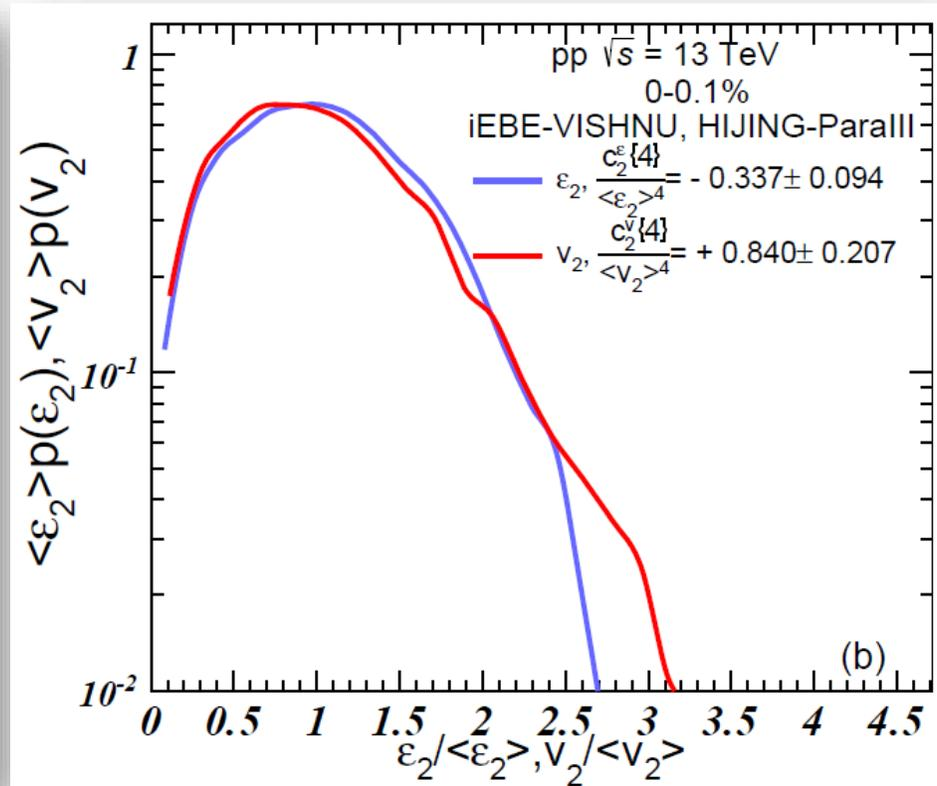
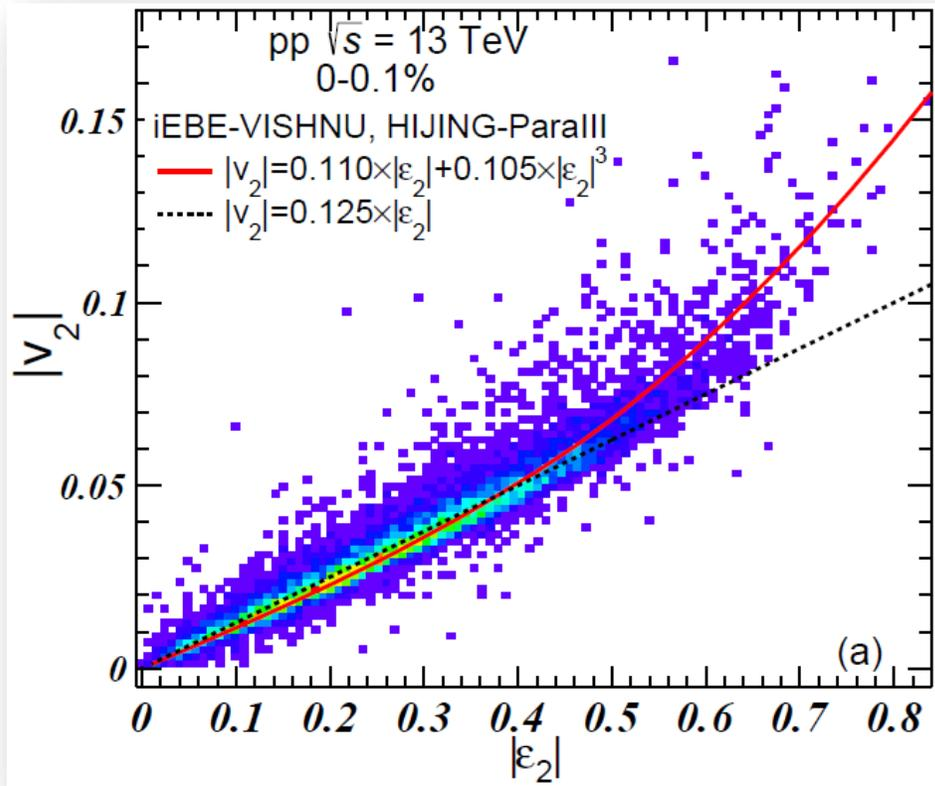
$$v_2\{4\} = (-c_2\{4\})^{\frac{1}{4}}$$

- To get the real value of $v_2\{4\}$, $c_2\{4\}$ should be negative.

W. Zhao, Y. Zhou, H. Xu, W. Deng and H. Song, Phys. Lett. B 780, 495 (2018)

- iEBE-VISHNU + HIJING cannot obtain the negative $c_2\{4\}$.

$P(v_2)$ and $P(\varepsilon_2)$ distributions: from $c_2^\varepsilon\{4\}$ to $c_2^v\{4\}$



$$C_2\{4\} = -2\langle v_2^2 \rangle^2 + \langle v_2^4 \rangle$$

$$= -\langle v_2 \rangle^4 + 2\sigma_{v_2}^2 \langle v_2^2 \rangle^2 + \sigma_{v_2}^2 (v_2 = \langle v_2 \rangle + \sigma_{v_2})$$

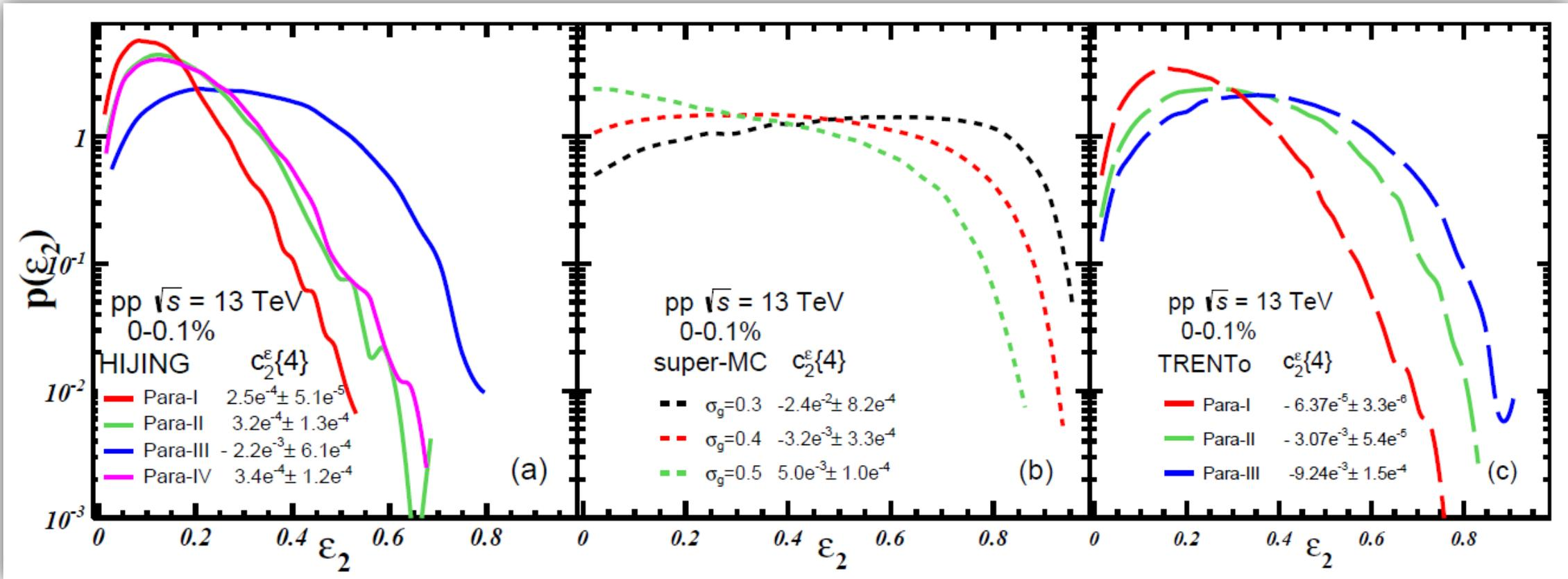
$$v_2\{4\} = (-C_2\{4\})^{\frac{1}{4}}$$

To get the real value of $v_2\{4\}$, $c_2\{4\}$ should be negative.

Linear term + cubic term fit: $|v_2| = 0.110 \times |\varepsilon_2| + 0.105 \times |\varepsilon_2|^3$ W. Zhao, Y. Zhou, K. Murase, and H. Song, arXiv:2001.06742.

- Small ε_2 , linear response is good; at large ε_2 , the cubic response is important.
- Certain deviations between $P(v_2/\langle v_2 \rangle)$ and $P(\varepsilon_2/\langle \varepsilon_2 \rangle)$.
- Leading to positive $C_2^v\{4\}$ in final states even with negative $C_2^\varepsilon\{4\}$ in initial state change.

Other initial models: HIJING, super-MC and TRENTo



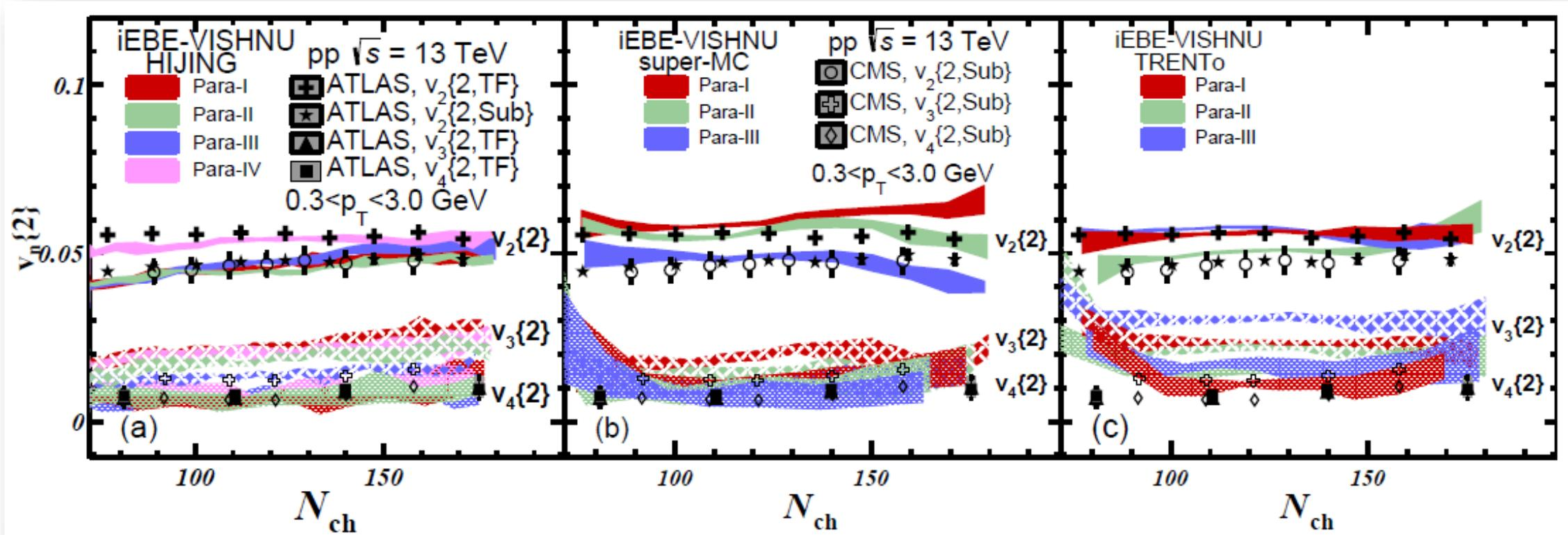
W. Zhao, Y. Zhou, K. Murase, and H. Song, arXiv:2001.06742.

K. Welsh, J. Singer, and U. W. Heinz, PRC 94,024919 (2016).

J. S. Moreland, J. E. Bernhard and S. A. Bass, PRC 101, 024911 (2020).

- Different shapes of $p(\epsilon_2)$ of HIJING, super-MC and TRENTo initial models.
- Some initial models get the negative $c_2^{\epsilon\{4\}} < 0$ in the initial state.

$v_n\{2\}$ calculated by HIJING, super-MC and TRENTo



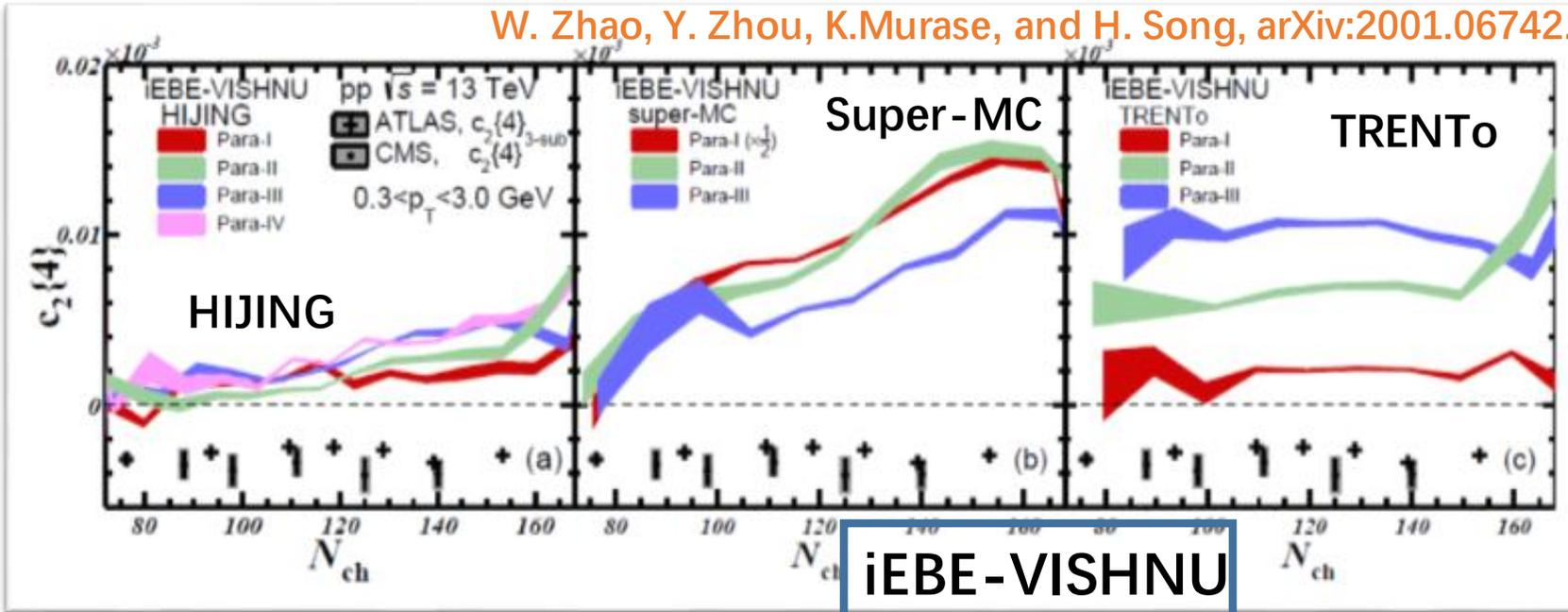
$$v_n\{2\} = \sqrt{\langle v_n^2 \rangle} = \sqrt{\langle v_n \rangle^2 + \sigma_{v_n}^2}, \quad (v_n = \langle v_n \rangle + \sigma_{v_n})$$

W. Zhao, Y. Zhou, K. Murase, and H. Song, arXiv:2001.06742.
ATLAS, Phys. Lett. B 789, 444 (2019).

- With properly turned parameters, iEBE-VISHNU + HIJING, super-MC and TRENTo can well describe the $v_2\{2\}$ and $v_4\{2\}$ of high multiplicity events in p-p system.
- Again, hydro simulations tend to overestimate the $v_3\{2\}$, which needs to be understood.

$c_2\{4\}$ from hydro with various initial conditions on market

W. Zhao, Y. Zhou, K. Murase, and H. Song, arXiv:2001.06742.



$$c_2\{4\} = -2\langle v_2^2 \rangle^2 + \langle v_2^4 \rangle$$

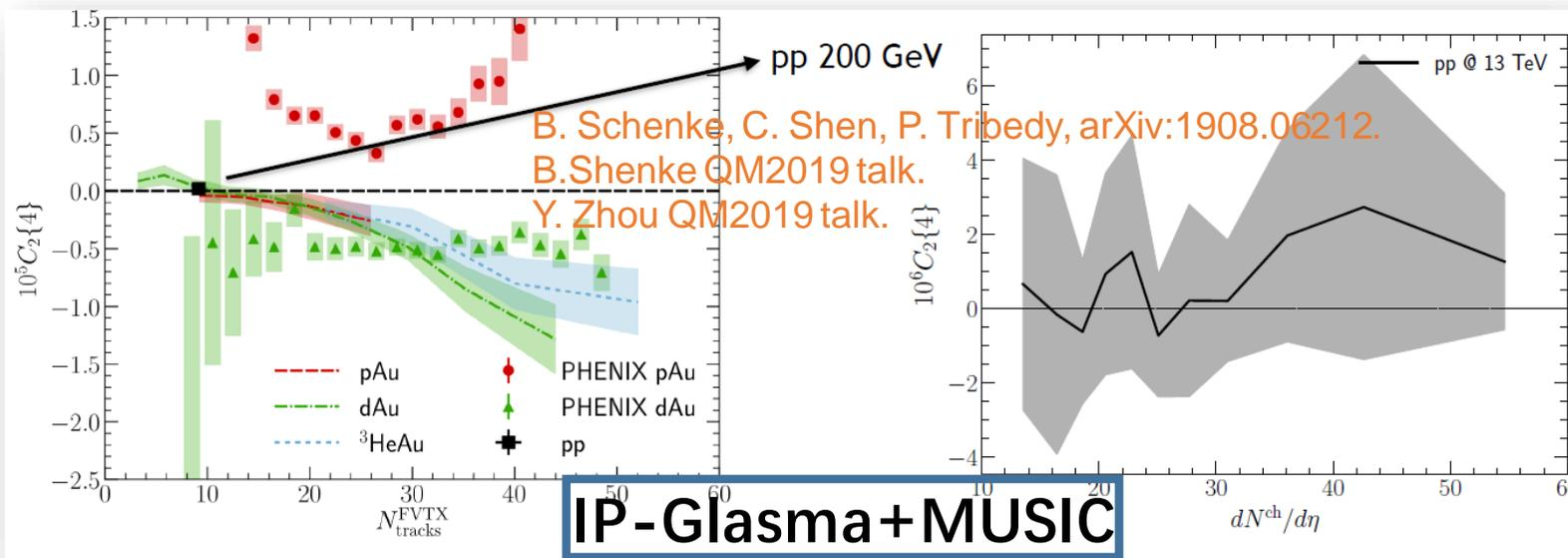
$$= -\langle v_2 \rangle^4 + 2\sigma_{v_2}^2 \langle v_2^2 \rangle^2 + \sigma_{v_2}^2 (v_2 = \langle v_2 \rangle + \sigma_{v_2})$$

$$v_2\{4\} = (-c_2\{4\})^{\frac{1}{4}}$$

- To get the real value of $v_2\{4\}$, $c_2\{4\}$ should be negative.

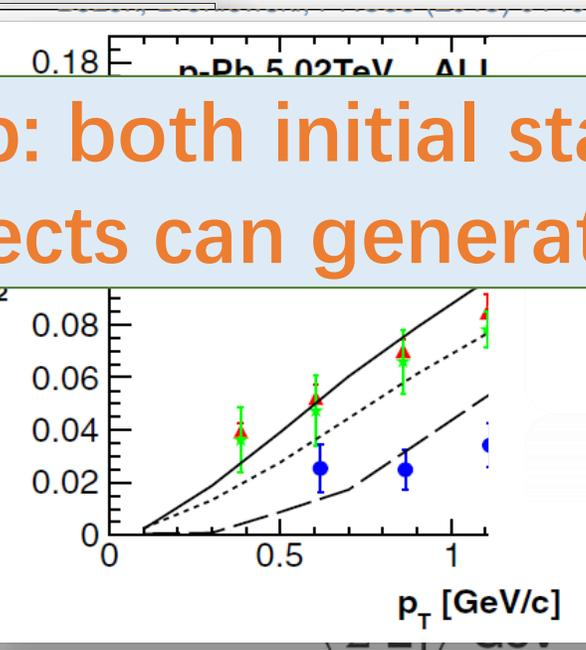
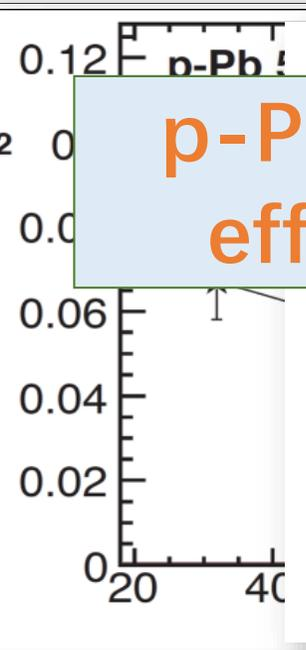
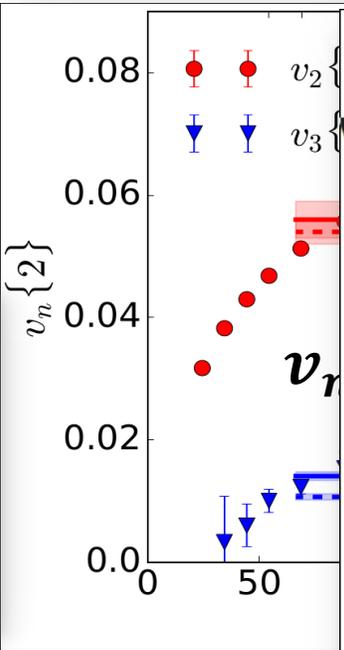
$c_2\{4\}$ puzzle in p-p collisions

- iEBE-VISHNU with various initial conditions cannot describe the negative $c_2\{4\}$.
- MUSIC with IP-Glasma also give positive $c_2\{4\}$ in pp collisions.

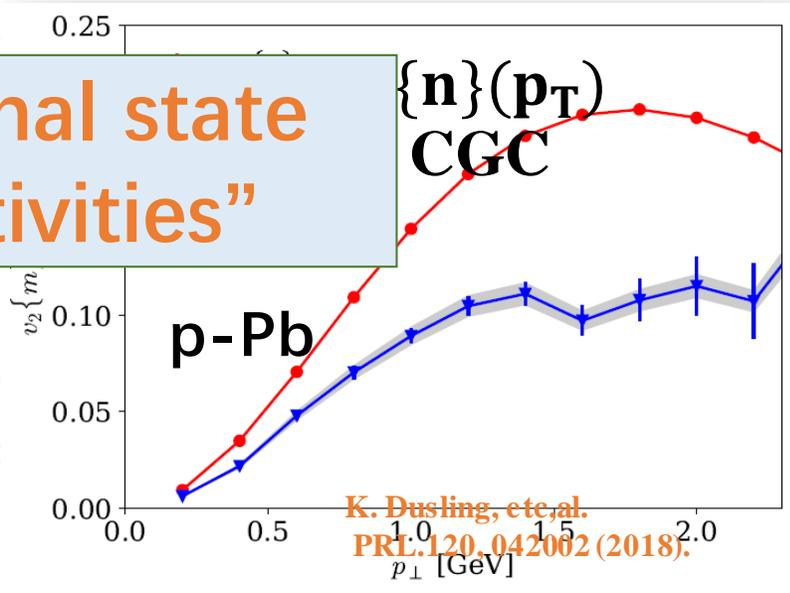


Short Summary for the collectivity in small systems at LHC

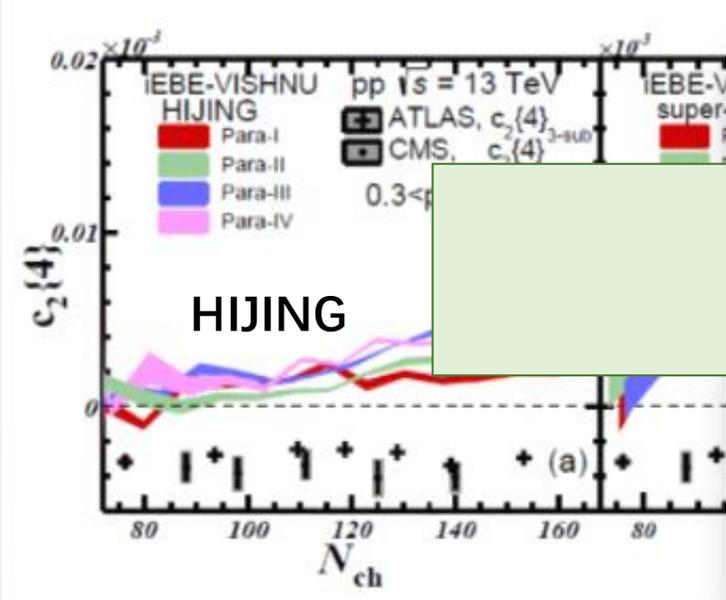
p-Pb: both initial state and final state effects can generate "collectivities"



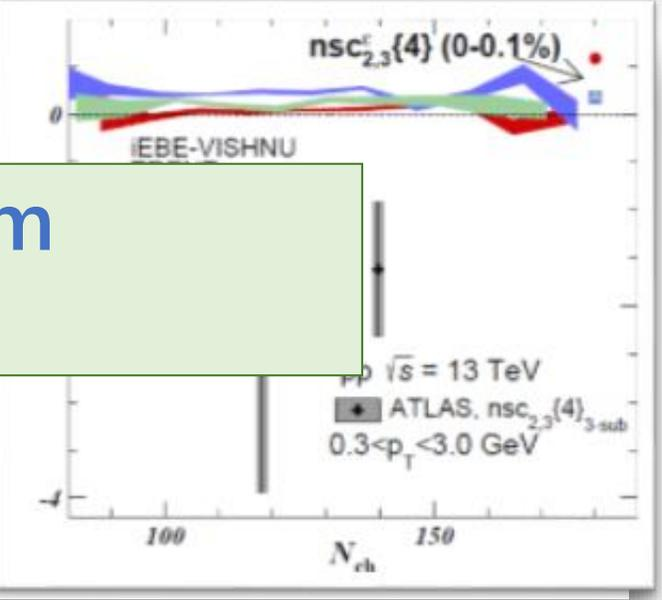
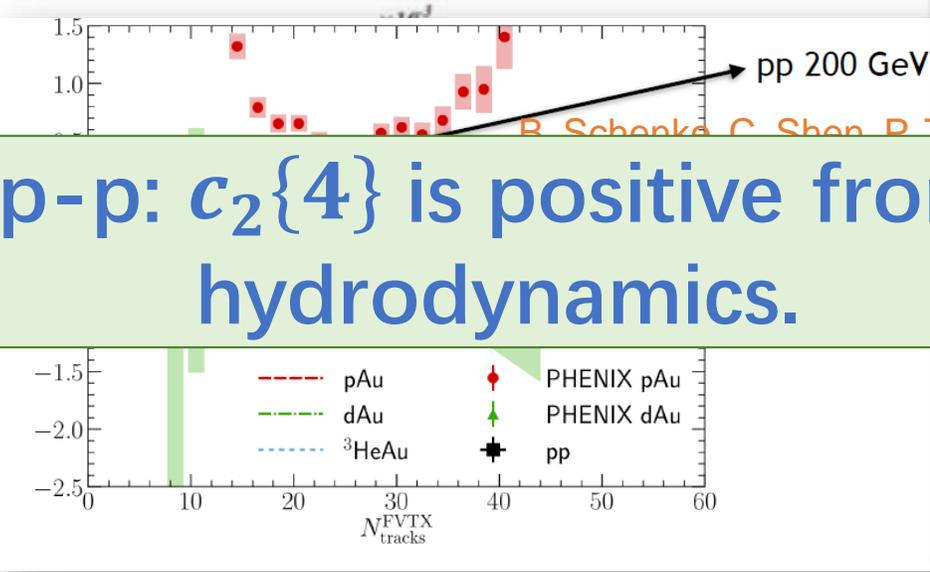
B.Schenke et al., PRL,117,162301(2016)



K. Dusling, et al. PRL,120,042002(2018).

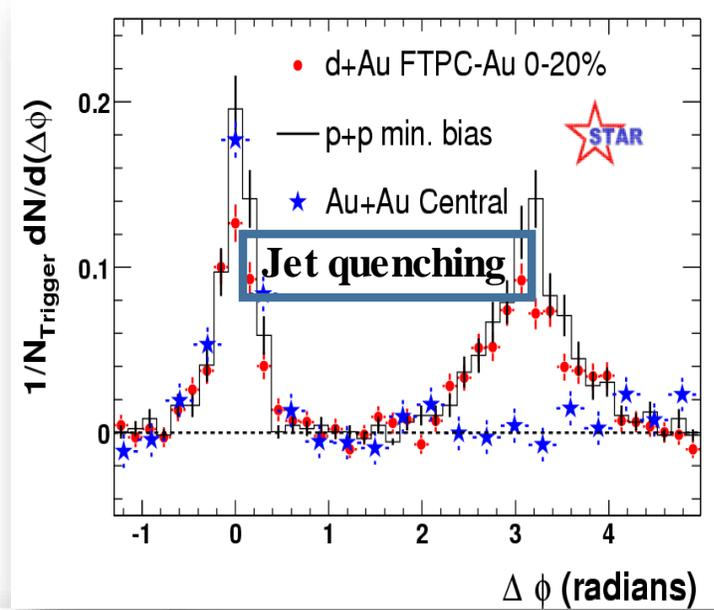


p-p: $c_2\{4\}$ is positive from hydrodynamics.

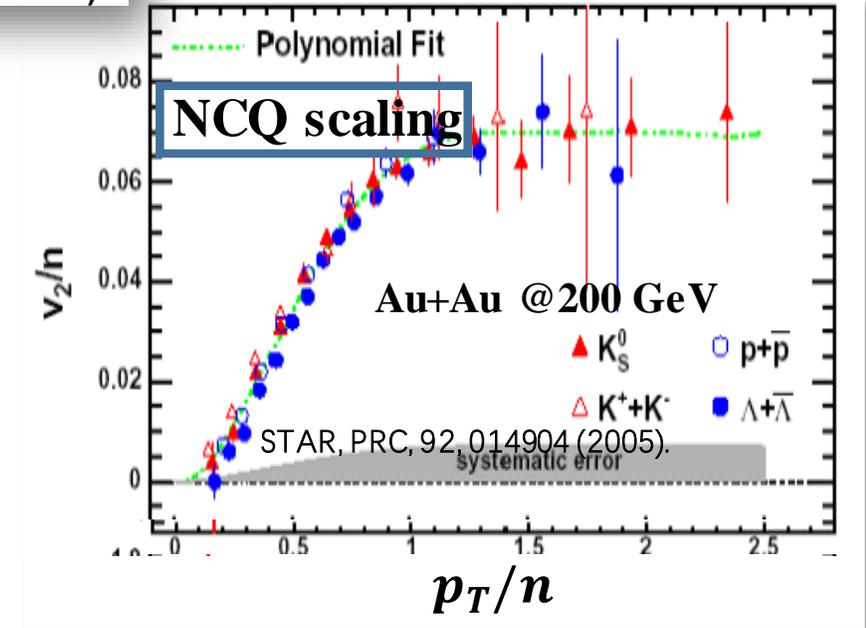
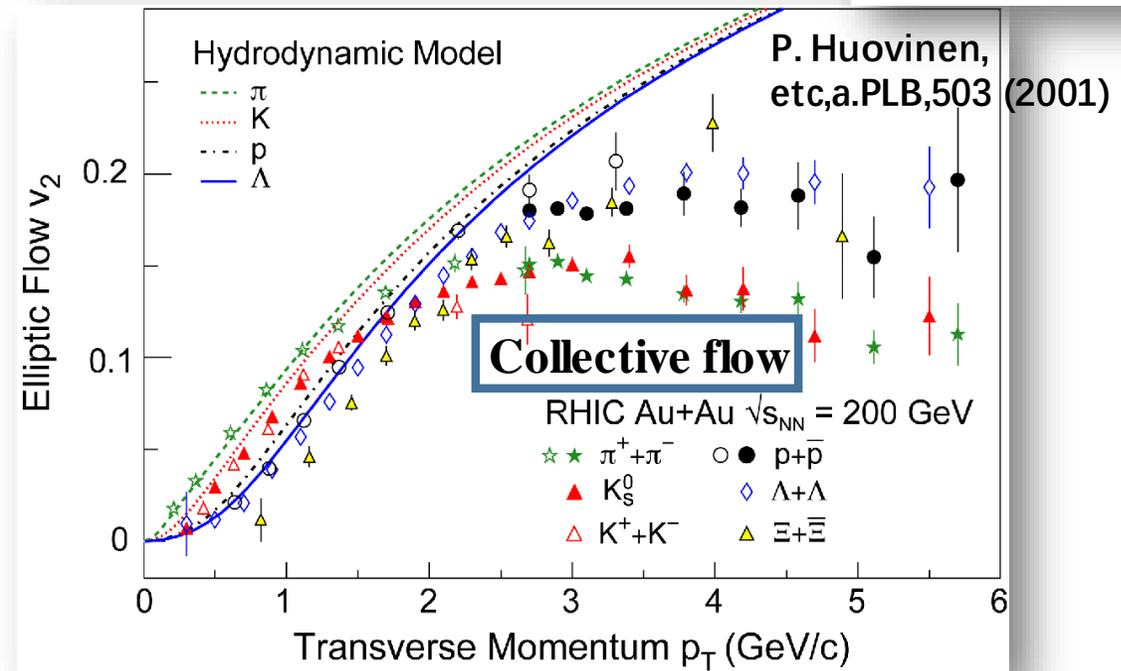


**Is QGP formed in the small systems?
(p-Pb collisions)**

Reminder: QGP signatures in heavy-ion collisions

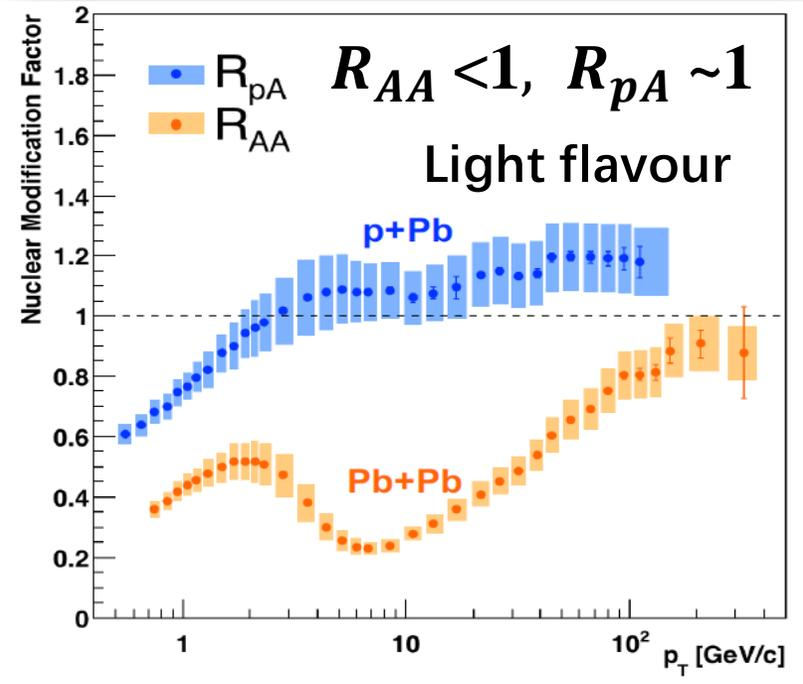


- It has been announced that QGP has been found at RHIC in heavy-ion collisions.

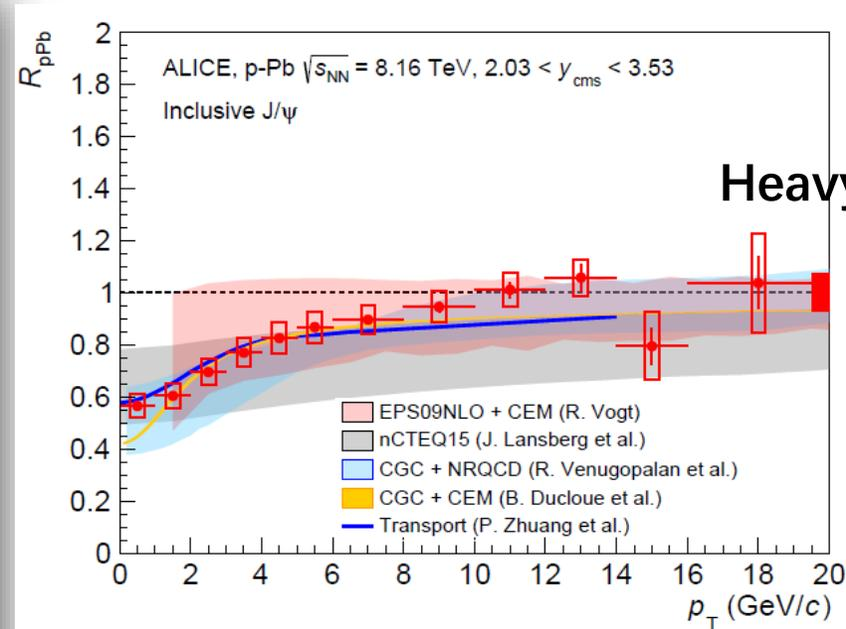


Related signatures in p-Pb system

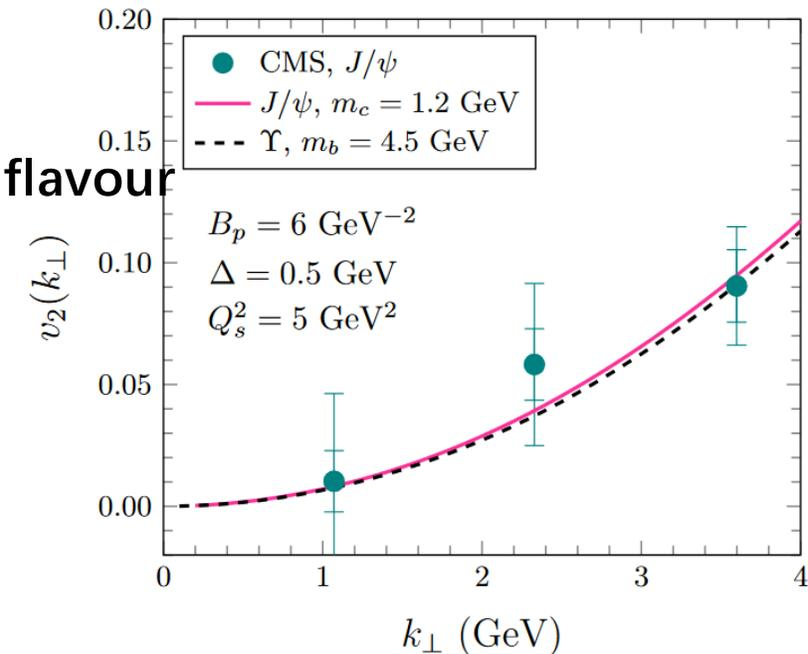
- Collective flow: Hydrodynamics or CGC initial states correlations?
- Hard Probes: no longer leave obvious hints due to the limited size and lifetime.



J.L.Nagle, et al. Ann.Rev. Nucl. Part. Sci 68,211 (2018)



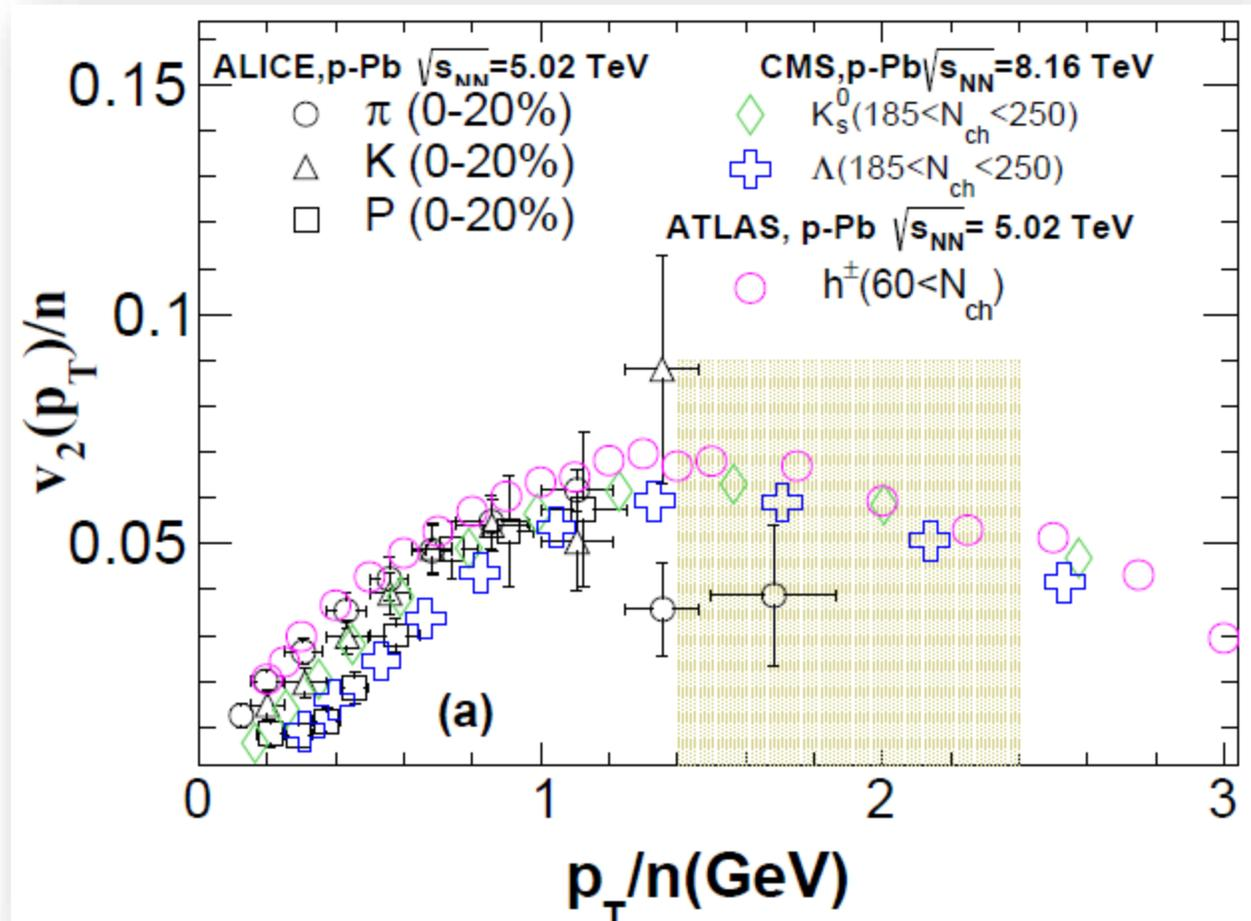
ALICE, JHEP 1807, 160 (2018)



C.Zhang, et al. PRL 122, 172302 (2019).

- R_{pA} of light hadrons and heavy flavor are consistent with one and compatible with cold nuclear effect in p-Pb collisions.
- $v_2(p_T)$ of heavy quark is also compatible with the CGC model calculations.

NCQ scaling in small system

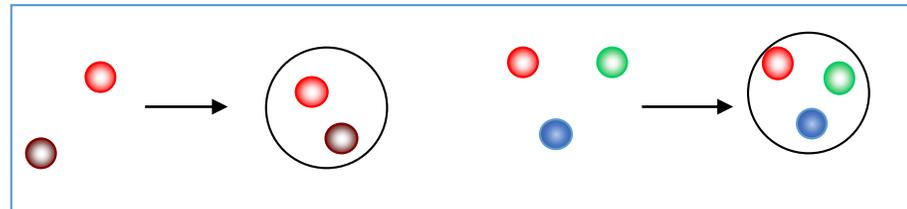
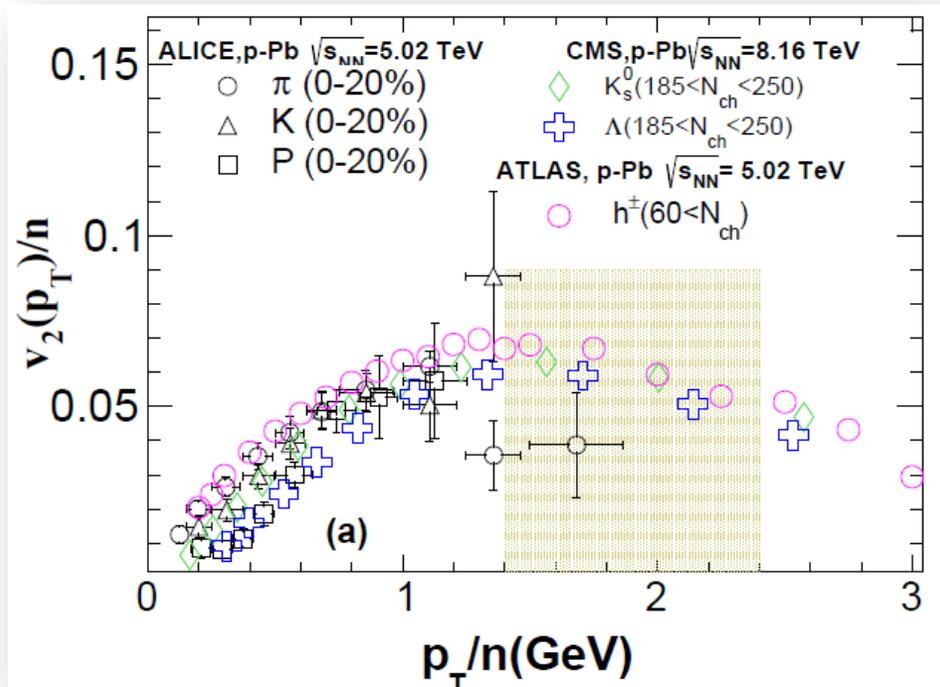


ALICE data: PLB, 726, 164 (2013).
CMS data: PRL, 121, 082301 (2018).
ATLAS data: PRC, 96, 024908 (2017).

- Observe the approximately NCQ scaling of v_2 at intermediate p_T in high multiplicity events of p-Pb collision in data.

Simple coalescence and NCQ scaling

- If hadrons' wave function has the form: $W_{M/B} \sim \delta(\mathbf{P} - \mathbf{p}_1 - \mathbf{p}_2)$ and quark exhibits the same elliptic flow: $f_a(\mathbf{p}_T) = \bar{f}_a(p_T) (1 + 2v_{2,q}(p_T) \cos 2\phi)$
- the meson's elliptic flow: $v_2^M(p_T) = \frac{2v_{2,q}(p_T/2)}{1+2v_{2,q}^2(p_T/2)} \sim 2v_{2,q}(p_T/2)$
- the baryon's elliptic flow: $v_2^B(p_T) = \frac{3v_{2,q}(p_T/3)}{1+6v_{2,q}^2(p_T/3)} \sim 3v_{2,q}(p_T/3)$



- NCQ scaling is important signal to probe partonic degree of freedom in small systems.

V.Greco, C. M. Ko and P. Levai, PRL 90, 202302 (2003).

R.J.Fries, B. Muller, C. Nonaka and S. A. Bass, PRL 90,202303 (2003).

D.Molnar and S.A.Voloshin, PRL 91, 092301 (2003).

Sophisticated Coalescence model

- Coalescence model

$$\frac{dN_M}{d^3\mathbf{P}_M} = g_M \int d^3\mathbf{x}_1 d^3\mathbf{p}_1 d^3\mathbf{x}_2 d^3\mathbf{p}_2 f_q(\mathbf{x}_1, \mathbf{p}_1) f_{\bar{q}}(\mathbf{x}_2, \mathbf{p}_2) \times W_M(\mathbf{y}, \mathbf{k}) \delta^{(3)}(\mathbf{P}_M - \mathbf{p}_1 - \mathbf{p}_2),$$

$$\frac{dN_B}{d^3\mathbf{P}_B} = g_B \int d^3\mathbf{x}_1 d^3\mathbf{p}_1 d^3\mathbf{x}_2 d^3\mathbf{p}_2 d^3\mathbf{x}_3 d^3\mathbf{p}_3 f_{q_1}(\mathbf{x}_1, \mathbf{p}_1) \times f_{q_2}(\mathbf{x}_2, \mathbf{p}_2) f_{q_3}(\mathbf{x}_3, \mathbf{p}_3) W_B(\mathbf{y}_1, \mathbf{k}_1; \mathbf{y}_2, \mathbf{k}_2) \times \delta^{(3)}(\mathbf{P}_B - \mathbf{p}_1 - \mathbf{p}_2 - \mathbf{p}_3),$$

Thermal & hard Partons:

- Thermal partons generated by hydro
- Hard partons generated by PYTHIA8, then suffered with energy loss by LBT

Coalescence processes:

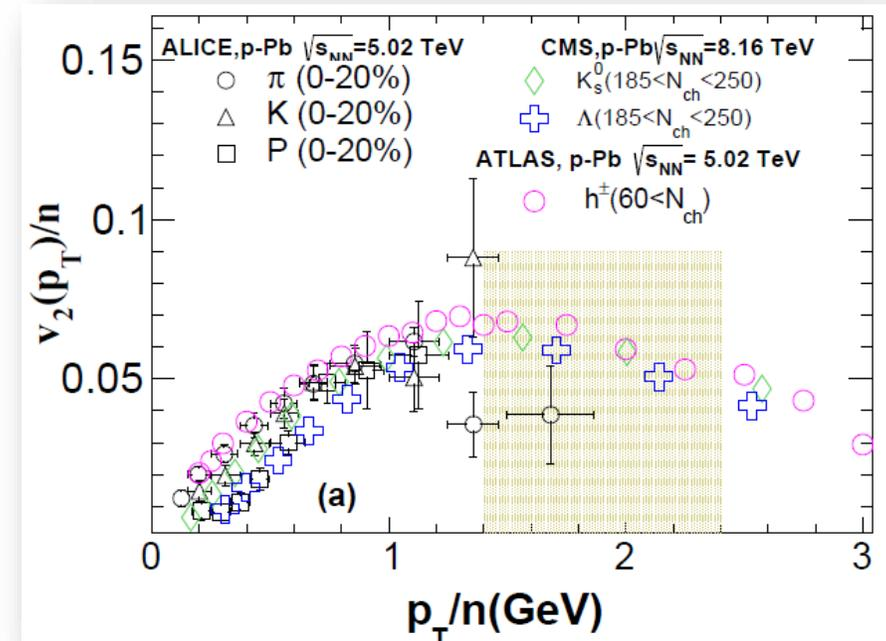
- thermal - thermal parton coalescence
- thermal - hard parton coalescence
- hard - hard parton coalescence

$g_{B(M)}$ is statistic factor, $f_{q/\bar{q}}$ is the phase-space distribution of (anti)quarks, $W_{M/B}$ is wigner function of meson(baryon).

Here, we use the harmonic oscillator for wave functions of hadrons, then do the Wigner transform to get the $W_{M/B}$.

Han, Fries and Ko, PRC 93, 045207 (2016).

Zhao, Ko, Liu, Qin and Song, arxiv:1911.00826.



Hydro-Coal-Frag Hybrid Model

Zhao, Ko, Liu, Qin and Song, arxiv:1911,00826.

Thermal hadrons (VISH2+1):

- generated by hydro. with Cooper-Frye.
- Meson: $p_T < 2p_{T1}$; baryon: $p_T < 3p_{T1}$.

Coalescence hadrons (Coal Model):

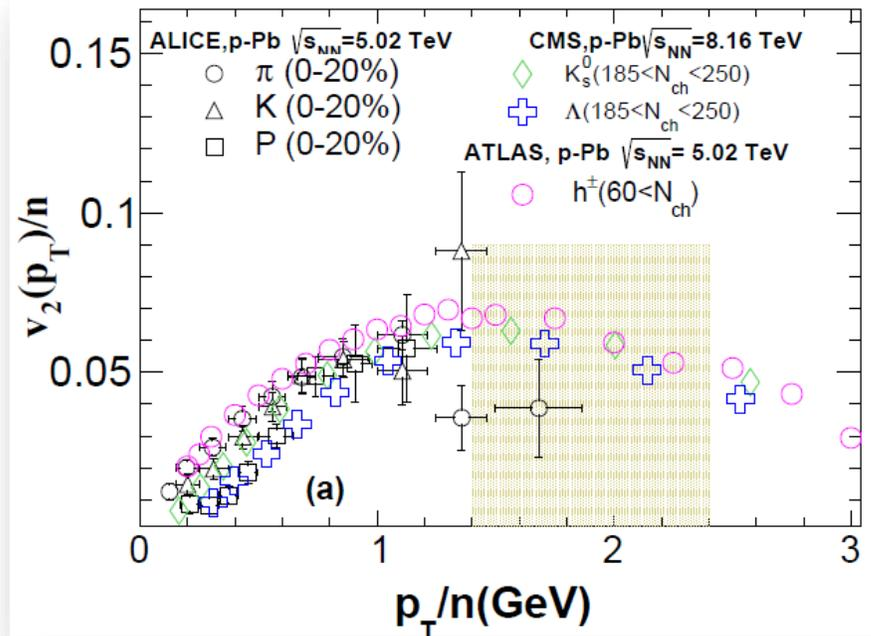
- generated by coalescence model including thermal-thermal, thermal-hard & hard-hard parton coalescence.

Fragmentation hadrons :

- the remnant hard quarks feed to fragmentation .

UrQMD afterburner:

- All hadrons are feed into UrQMD for hadronic evolution, scatterings and decays



Hydro. Coalescence, fragmentation fragmentation

0

3GeV

5GeV

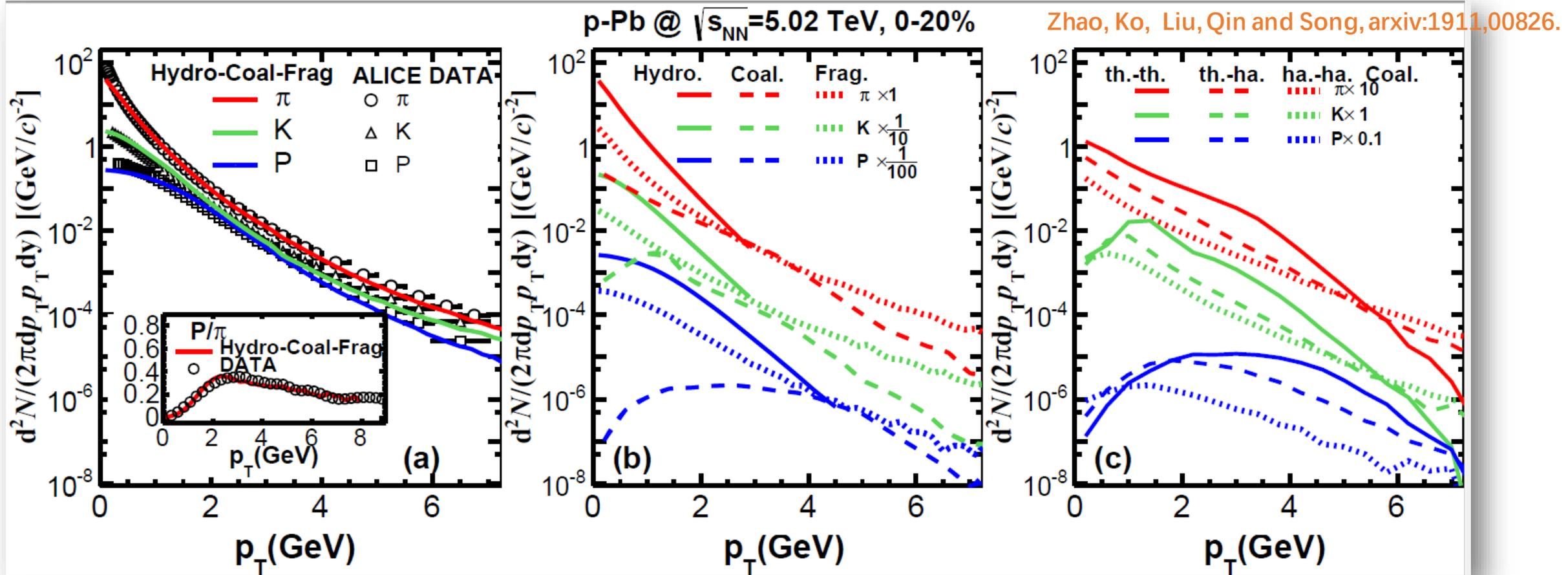
P_T

Main Parameters:

- Thermal partons from hydro with $p_T > p_{T1}$.
- Hard partons from LBT with $p_T > p_{T2}$

Fixed by the p_T spectra, with $p_{T1} = 1.6$ GeV and $p_{T2} = 2.6$ GeV

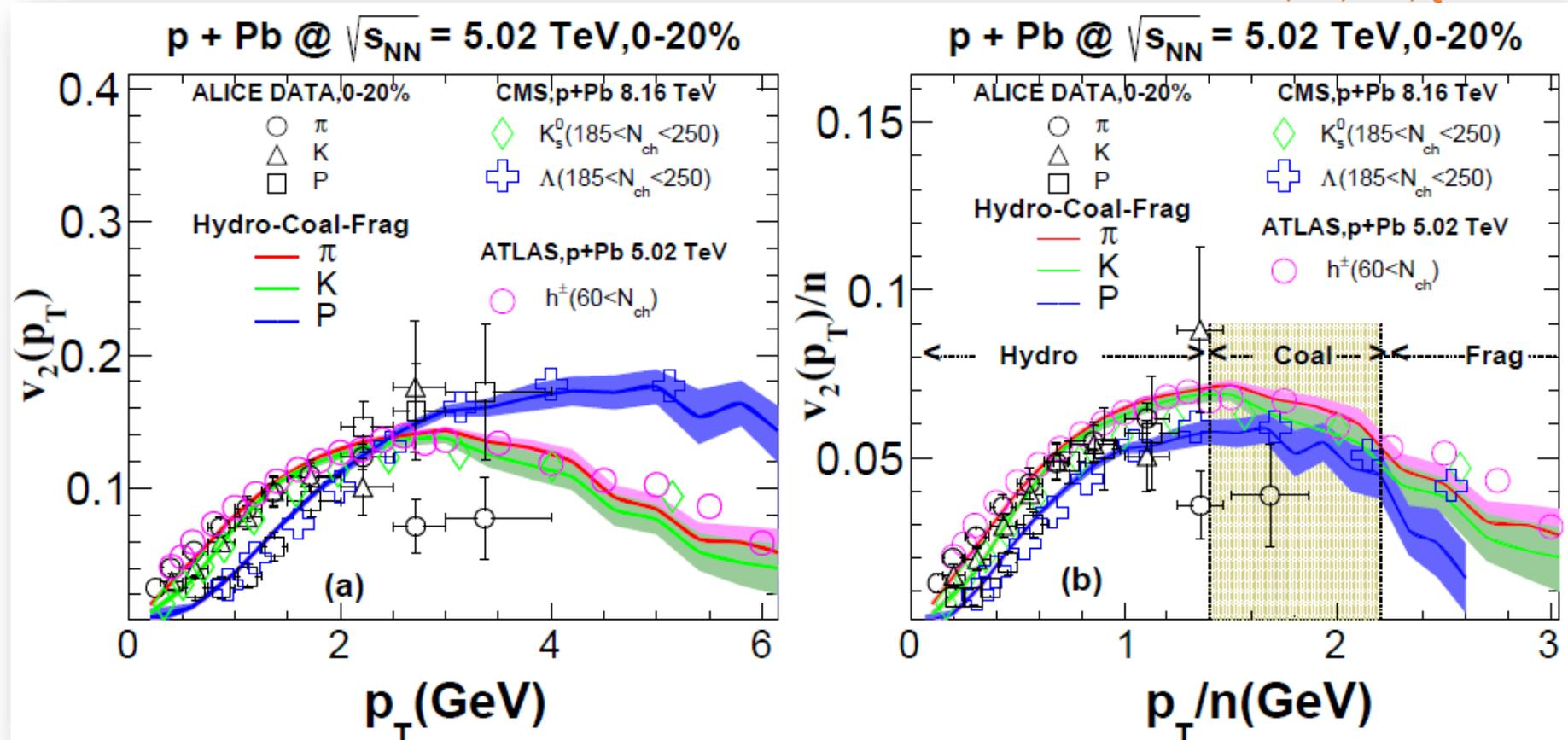
Spectra, and Hydro. Coal. and Frag. contributions



- Hydro-Coal-Frag hybrid model well describe the spectra and P/π at 0-8 GeV.
- Hydro. dominates at low p_T , at inter-mediate p_T , coal. and frag. both have contributions. Fragmentation dominates high p_T . Three processes smoothly merge at intermediate p_T .
- Coalescence hadrons: Thermal-thermal coalescence dominates at intermediate p_T .

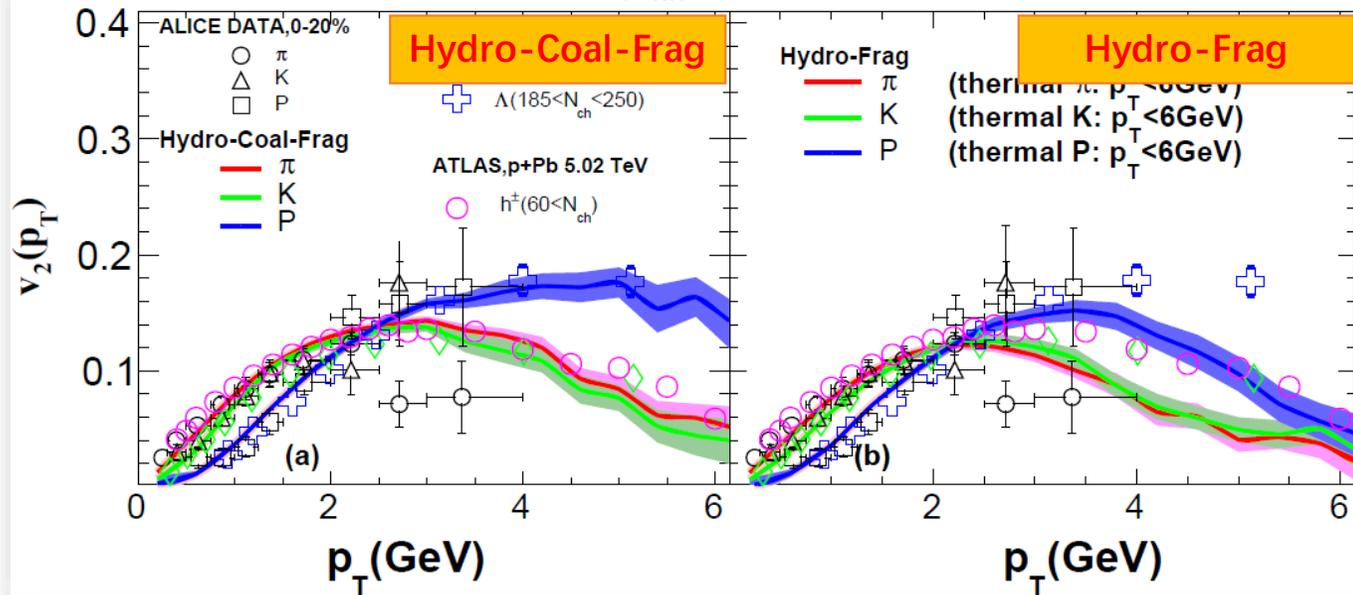
$v_2(p_T)$ and NCQ scaling

Zhao, Ko, Liu, Qin and Song, arxiv:1911.00826.



- Combine hydro and jet with coalescence and fragmentation, Hydro-Coal-Frag model can well describe the $v_2(p_T)$ of π , K and P within p_T range of 0-6 GeV.
- At intermediate p_T , Hydro-Coal-Frag model can get the approximately NCQ scaling of π , K and P of v_2 as the data shown.

p + Pb @ $\sqrt{s_{NN}} = 5.02$ TeV, 0-20%

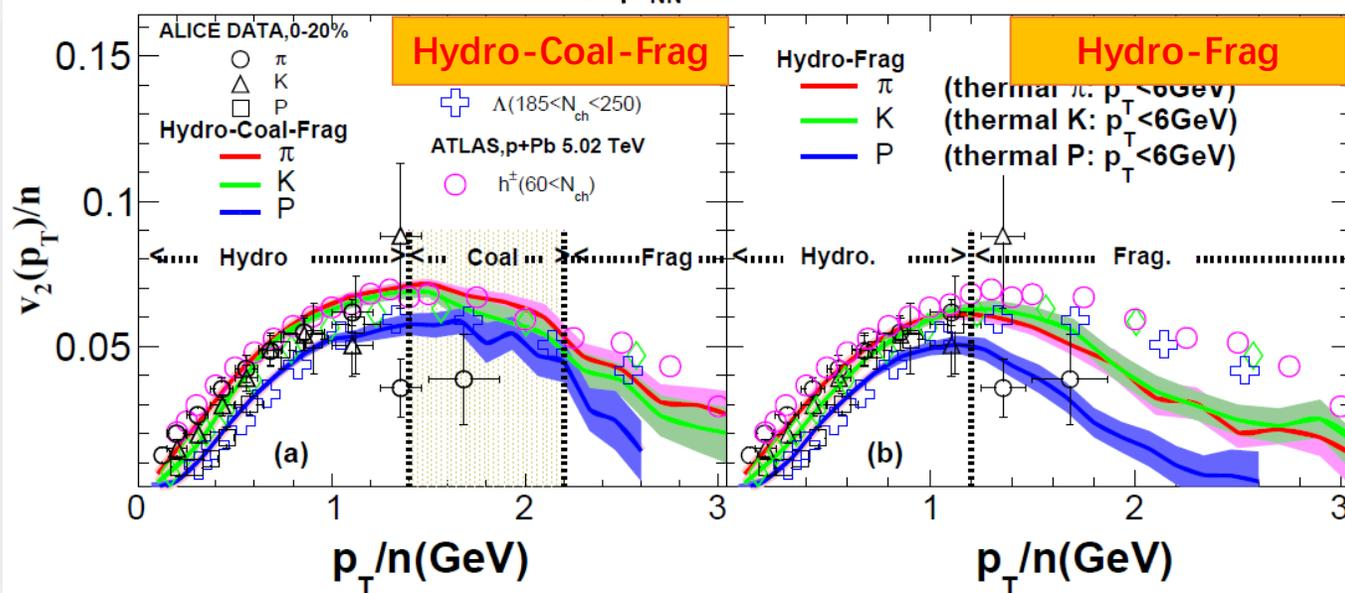


Zhao, Ko, Liu, Qin and Song, arxiv:1911.00826.

The importance of quark coalescence in p-Pb collisions

- Without coalescence, Hydro-Frag greatly underestimates the $v_2(p_T)$ at intermediate p_T
- Without coalescence, Hydro-Frag will also greatly violate the NCQ scaling at intermediate p_T , with the deviation of NCQ scaling at the level of $\pm 50\%$.

p + Pb @ $\sqrt{s_{NN}} = 5.02$ TeV, 0-20%



Summary

Pb+Pb Collisions at the LHC

- Hydrodynamics has the strong predictive power for the various flow data in heavy-ion collisions.
- The η/s and ζ/s have been extracted by the Bayesian global fitting.

p+Pb Collisions at the LHC

- Many flow observables have been quantitatively/qualitatively described by hydro, supporting the collective expansion in p-Pb collisions.
- Coalescence model calculations nicely described NCQ scaling of v_2 at intermediate p_T , strongly hint the partonic degrees of freedom in high multiplicity p-Pb collision.

p+p Collisions at the LHC

- The sign of $c_2\{4\}$ is still a puzzle for hydro with various initial conditions on market.
- More flow observables are still needed to be measured

It is important to investigate **why hydro works & when and where it works ?**

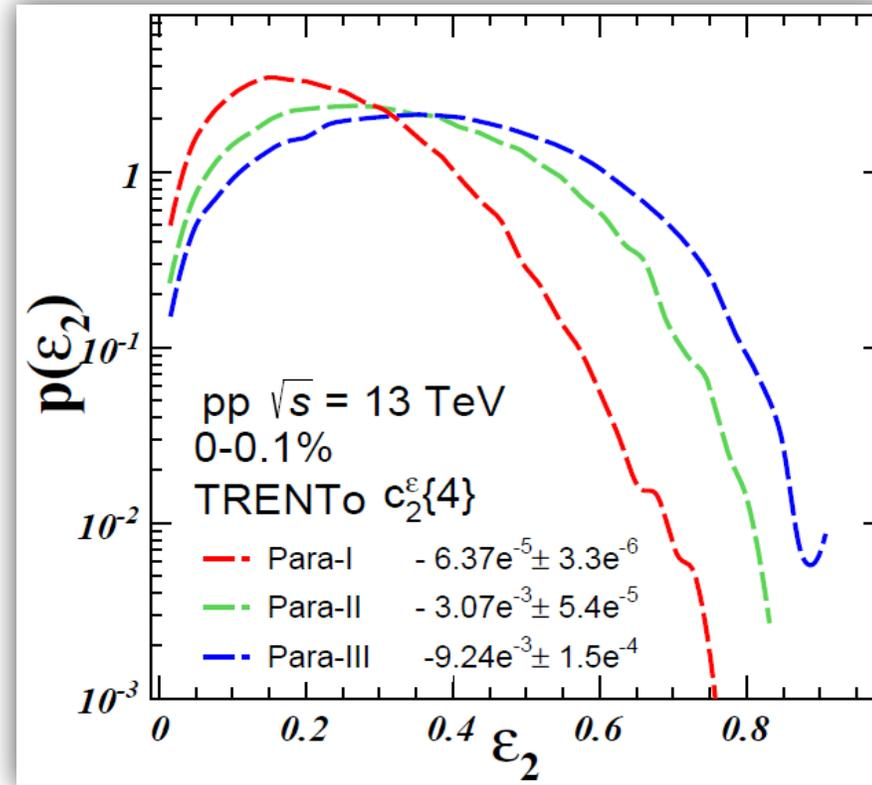
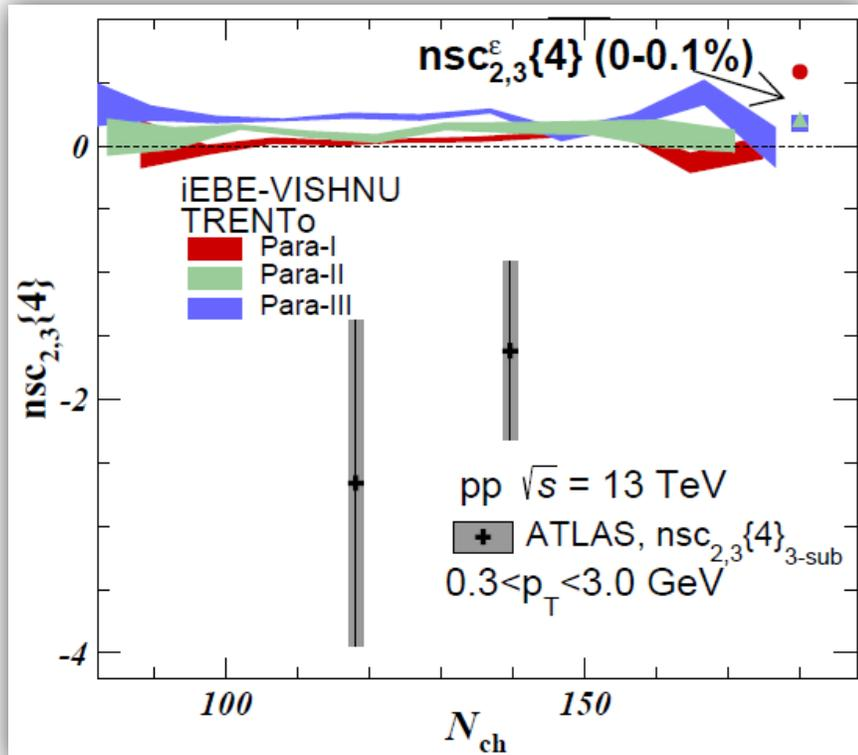
Thanks

THANKS

Back Up

back up

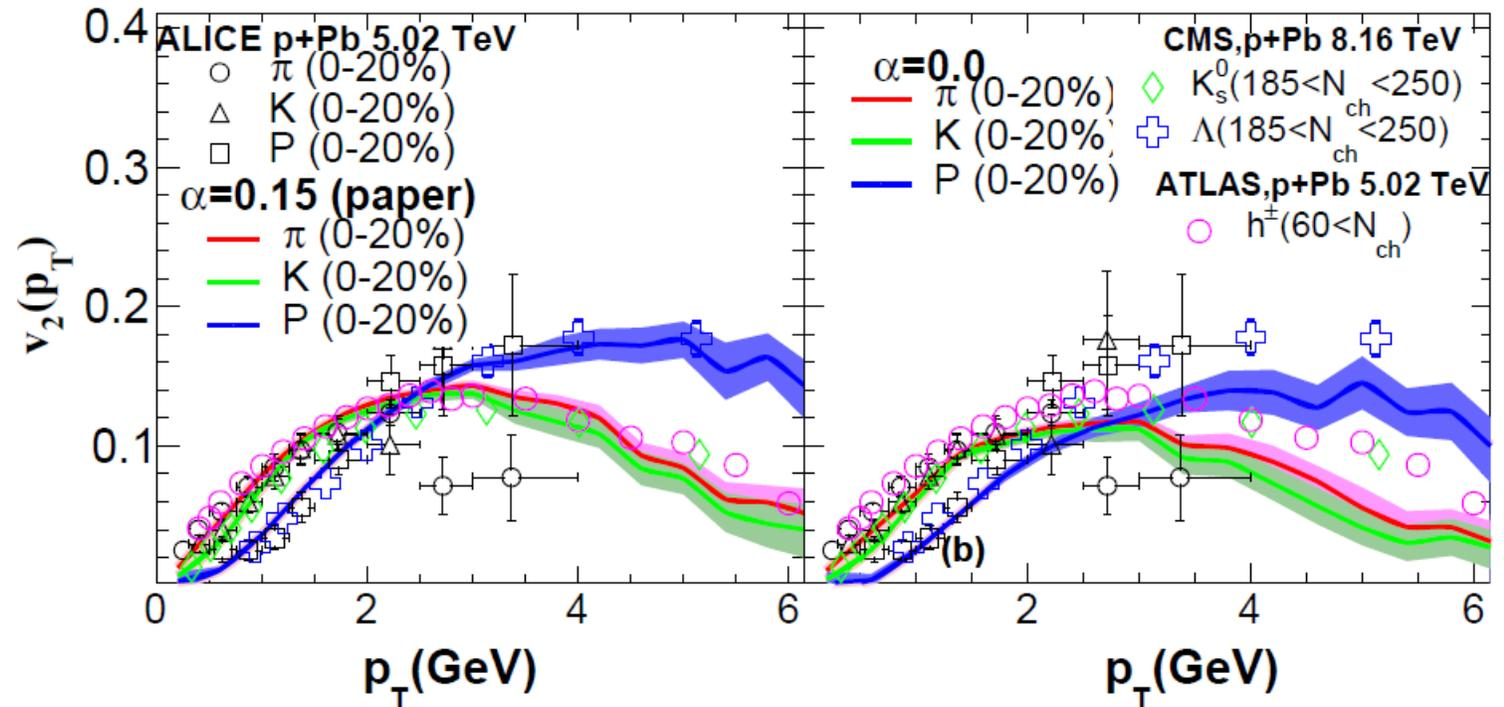
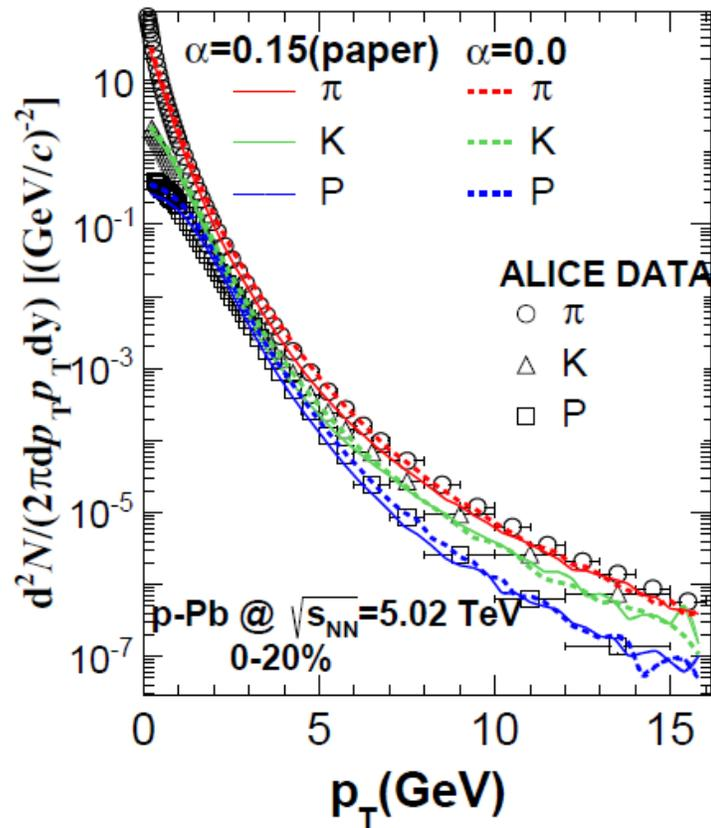
More comments: non-linear response's effects on Symmetric-Cumulant



W. Zhao, Y. Zhou, K. Murase, and H. Song, arXiv:2001.06742.

- If $v_2 \propto \epsilon_2$ and $v_3 \propto \epsilon_3$, then $nsc_{2,3}^v\{4\} = nsc_{2,3}^\epsilon\{4\}$.
- In hydro simulations, $nsc_{2,3}^v\{4\}$ in the final states keep the same sign of the initial states correlations $nsc_{2,3}^\epsilon\{4\}$. But the hierarchy changes, Para-I > Para-II \approx Para-III for initial states, but Para-III > Para-II > Para-I for the final states. This is caused by different non-linear response effects with different shapes of $P(\epsilon_2)$.

Check α_s effects in p-Pb collisions



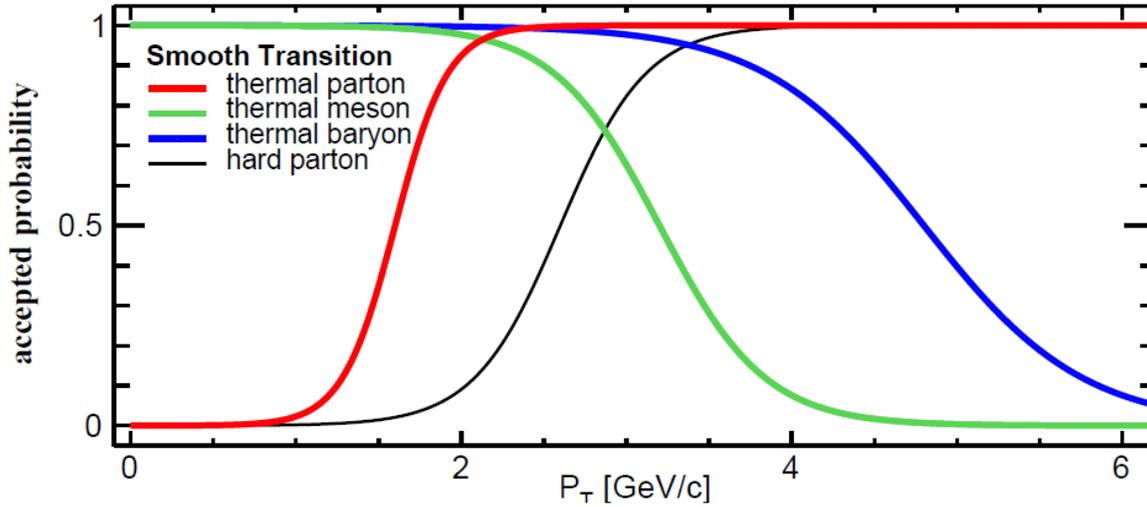
S. Cao, T. Luo, G. Y. Qin and X. N. Wang, PRC 94,014909 (2016).

Zhao, Ko, Liu, Qin and Song, arxiv:1911.00826.

Zhao, Ko, Liu, Qin and Song, in preparation.

- The effective coupling constant α_s in the LBT model controls the energy loss effect when hard parton traversing the medium.
- Changing $\alpha_s=0.15$ to $\alpha_s=0.0$ increase p_T -spectra of π , K and P by about 40% for $p_T > 3$ GeV and has negligible effects for $p_T > 8$ GeV. It also decreases the $v_2(p_T)$ of π , K and P for $p_T > 3$ GeV, where the fragmentation contribution gradually becomes important.

Smooth transition of p_{T1} and p_{T2}

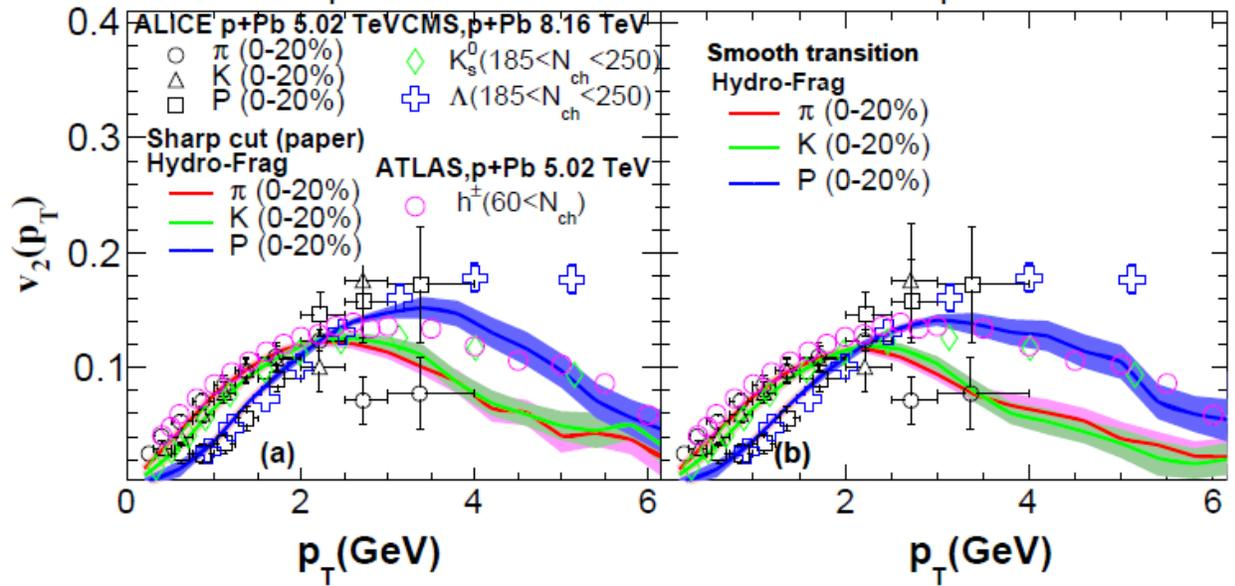
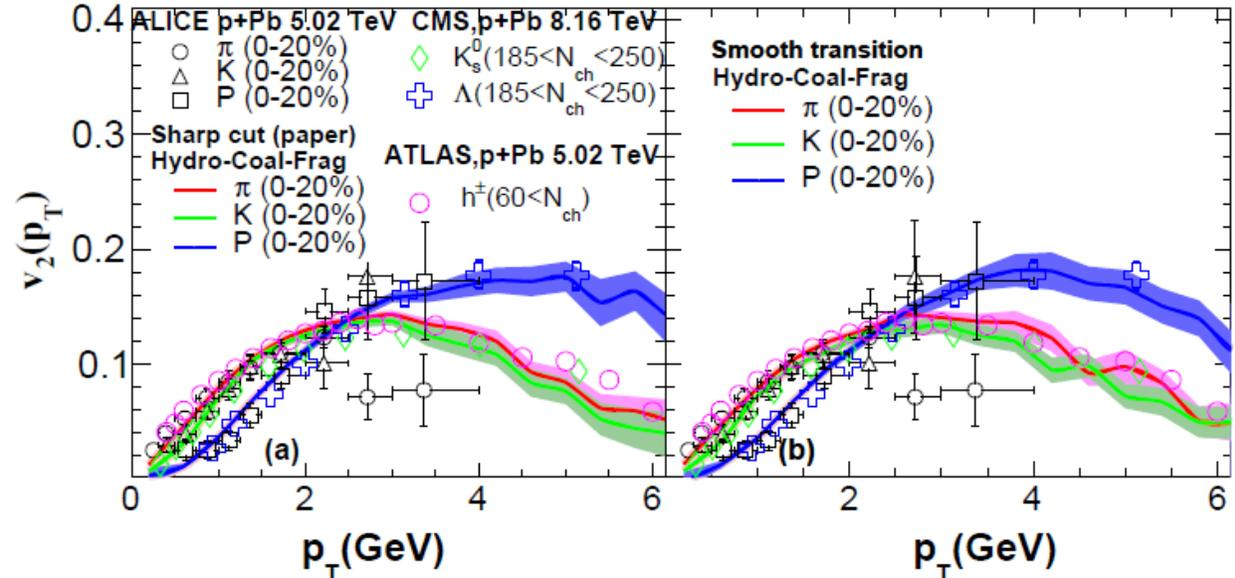


$$P_{\text{thermal/hard parton}} = \frac{\tanh[5(p_T - p_{T0})/p_{T0}] + 1}{2},$$

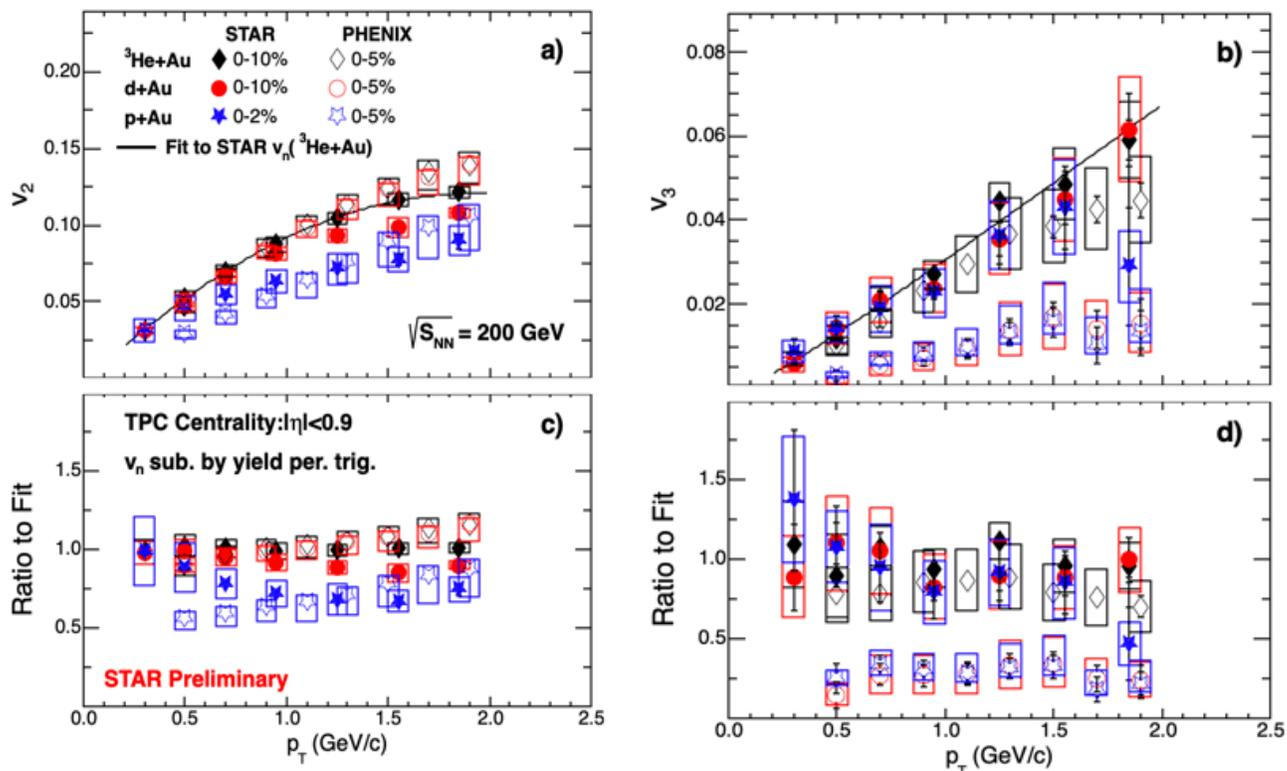
$$P_{\text{thermal hadrons}} = 1 - \frac{\tanh[5(p_T - p_{T0})/p_{T0}] + 1}{2}$$

- Using a smooth transitions in the p_T spectra for thermal and hard partons gives the same results with a sharp cut.

Zhao, Ko, Liu, Qin and Song, arxiv:1911.00826.
 Zhao, Ko, Liu, Qin and Song, in preparation.



Comparison of PHENIX and STAR $v_n(p_T)$ measurements for p/d/ ^3He +Au



- The STAR and PHENIX measurements for v_2 are in reasonable agreement for all systems
 - ✓ System-dependent trends consistent with “shape-size” dependencies
- The STAR and PHENIX v_3 measurements for p/d+Au differ by more than a factor of 3
 - ✓ System independent STAR v_3
 - ✓ System dependent PHENIX v_3

PHENIX: PRC95, 034910, Nature Physics 15, 214–220

PHENIX EP	^3He +Au	d+Au	p+Au
(ψ_2^{BPCS})	0.110 ± 0.0050	0.1073 ± 0.0003	0.062 ± 0.003
(ψ_3^{BPCS})	0.034 ± 0.0051	0.0565 ± 0.0097	0.067 ± 0.009

Note:
 ✓ EP resolution is proportional to v_n and \sqrt{N} !

$$v_n(EP) = \frac{v_n^{obs}}{\psi_n}$$

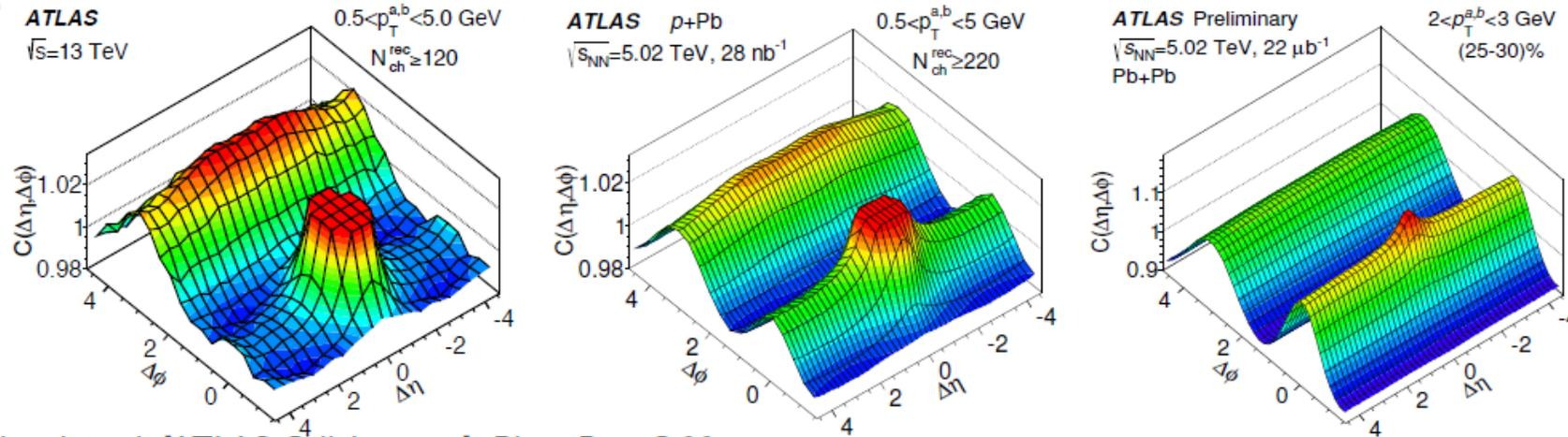
v_n^{obs} is the observed harmonic.
 ψ_n is the Event-Plane resolution;
 Poskanzer and Voloshin, PRC, 58, 1671 (1998).

- p-Au, 0-5%, $\langle \frac{dN_{ch}}{d\eta} \rangle = 12.3 \pm 1.7$
- d-Au, 0-5%, $\langle \frac{dN_{ch}}{d\eta} \rangle = 18.6 \pm 1.5$
- ^3He +Au, 0-5%, $\langle \frac{dN_{ch}}{d\eta} \rangle = 23.6 \pm 2.5$

PHENIX, PRL 121, 222301 (2018).

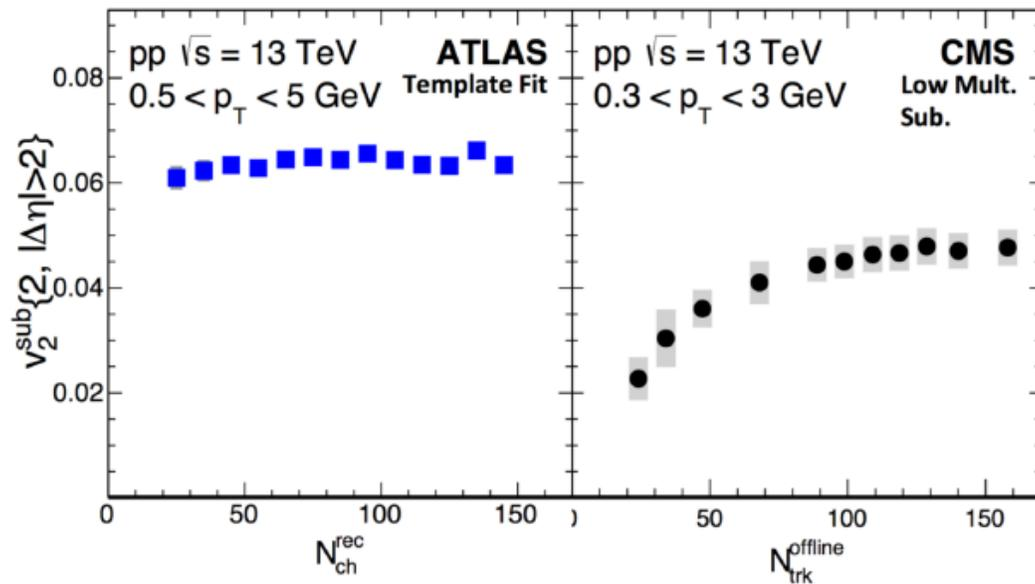
- The STAR measurements are consistent with the important role of “size” (N_{ch}) in addition to the fluctuations-driven eccentricity ($\epsilon_{2,3}$)
 - ✓ This observation is consistent with recent hydrodynamic calculations which incorporates nucleonic substructure

2-particle correlation in p-p collisions



M. Aaboud *et al.* [ATLAS Collaboration], Phys. Rev. C **96**, no. 2, 024908

- Two-particle correlations in p-p:



- Similar double ridge structure, but with smaller magnitudes in p-p collisions.
- Peripheral subtraction (CMS): $v_{n,n}^{peri} \approx 0$
- Template fit (ATLAS): $v_{n,n}^{cent} \approx v_{n,n}^{peri}$

Beyond fluid dynamics?

Flow in AA and pA as an interplay of fluid-like and non-fluid like excitations

Aleksi Kurkela,^{1,2,*} Urs Achim Wiedemann,^{1,†} and Bin Wu^{1,‡}

¹*Theoretical Physics Department, CERN, CH-1211 Genève 23, Switzerland*

²*Faculty of Science and Technology, University of Stavanger, 4036 Stavanger, Norway*

To study the microscopic structure of quark-gluon plasma, data from hadronic collisions must be confronted with models that go beyond fluid dynamics. Here, we study a simple kinetic theory model that encompasses fluid dynamics but contains also particle-like excitations in a boost invariant setting with no symmetries in the transverse plane and with large initial momentum asymmetries. We determine the relative weight of fluid dynamical and particle like excitations as a function of system size and energy density by comparing kinetic transport to results from the 0th, 1st and 2nd order gradient expansion of viscous fluid dynamics. We then confront this kinetic theory with data on azimuthal flow coefficients over a wide centrality range in PbPb collisions at the LHC, in AuAu collisions at RHIC, and in pPb collisions at the LHC. Evidence is presented that non-hydrodynamic excitations make the dominant contribution to collective flow signals in pPb collisions at the LHC and contribute significantly to flow in peripheral nucleus-nucleus collisions, while fluid-like excitations dominate collectivity in central nucleus-nucleus collisions at collider energies.

**A. Kurkela, U. A. Wiedemann and B. Wu, EPJC 79, no. 11, 965 (2019).
Jamie Nagle QM 2019.**

- Non-hydrodynamic excitations dominate in small systems?

Wigner functions of hadrons

To guarantee positive value of Wigner function for stable Monte Carlo sampling, the Wigner function replaced by the overlap of hadron Wigner function W_M with parton's Wigner function, $W_{q,\bar{q}}$:

$$\begin{aligned} \overline{W}_M(\mathbf{y}, \mathbf{k}) &= \int d^3\mathbf{x}'_1 d^3\mathbf{k}'_1 d^3\mathbf{x}'_2 d^3\mathbf{k}'_2 \\ &\times W_q(\mathbf{x}'_1, \mathbf{k}'_1) W_{\bar{q}}(\mathbf{x}'_2, \mathbf{k}'_2) W_M(\mathbf{y}', \mathbf{k}'). \end{aligned} \quad (3)$$

Using harmonic oscillator for wave functions of excited states of hadrons,

$$\phi_n(x) = \left(\frac{m\omega}{\pi\hbar}\right)^{1/4} \frac{1}{\sqrt{2^n n!}} H_n(\xi) e^{-\xi^2/2}, \quad (4)$$

$\xi = \sqrt{\frac{m\omega}{\hbar}}x$, $H_n(\xi)$ are Hermite polynomials, ω is the oscillator frequency.

K. C. Han, R. J. Fries and C. M. Ko, Phys. Rev. C 93, no. 4, 045207 (2016).

Wigner functions of hadrons

The quark wave function to be Gaussian wave packet, the wigner function of a meson in n -th excited state is

$$\overline{W}_{M,n}(\mathbf{y}, \mathbf{k}) = \frac{v^n}{n!} e^{-v}. \quad (5)$$

with

$$v = \frac{1}{2} \left(\frac{\mathbf{y}^2}{\sigma_M^2} + \mathbf{k}^2 \sigma_M^2 \right). \quad (6)$$

Similarly, the Gaussian smeared Wigner function for baryon is:

$$\overline{W}_{B,n_1,n_2}(\mathbf{y}_1, \mathbf{k}_1; \mathbf{y}_2, \mathbf{k}_2) = \frac{v_1^{n_1}}{n_1!} e^{-v_1} \cdot \frac{v_2^{n_2}}{n_2!} e^{-v_2}, \quad (7)$$

with

$$v_i = \frac{1}{2} \left(\frac{\mathbf{y}_i^2}{\sigma_{Bi}^2} + \mathbf{k}_i^2 \sigma_{Bi}^2 \right), \quad i = 1, 2. \quad (8)$$